the medial frontal area. The skin incision is made along the course of the parietal branch of the STA and extended upward to the midline near the bregma and then along the midline downward to the hairline (Fig. 1A). Using this larger skin flap, a longer portion of the frontal branch of the STA can be dissected which is adequate to reach the medial frontal area. The temporal muscle is separated as widely as possible. The galea of the frontal skin flap is also dissected, preserving a small vascular pedicle from the frontal branch of the STA (Fig. 1B). The normal frontotemporal craniotomy is performed, which can be covered with the temporal muscle flap, preserving the middle meningeal artery. The medial frontal craniotomy, which should be matched to the size of the galeal flap, is made separately (Fig. 1C). A larger craniotomy might be lead to less favorable cosmetic results. These two separate craniotomies preserve a bridge along the linear temporalis, and thus can retain the original shape of the skull.

The dura is then opened to preserve the main branch of the middle meningeal artery. Special attention is needed to avoid injury to the frontal cortical veins draining into the superior sagittal sinus. Selection of the branch of the ACA to act as recipient of the STA-ACA bypass is sometimes difficult. The area under the medial frontal craniotomy is the border zone between the ACA and MCA territories. We select a branch of the ACA passing upward from the interhemispheric fissure as the recipient. The frontal branch of the STA is then dissected very carefully to reach the recipient artery. The STA-ACA anastomosis is performed in an end-to-side fashion (Fig. 1D). STA-ACA bypass is technically more difficult than STA-MCA bypass, because the diameters of the anastomosed vessels are smaller. One or two STA-MCA bypasses are also established using other branches of the STA (Fig. 1D).

EDAMS is then performed in the usual way to cover the lateral craniotomy, and EGAS to cover the dural opening of the medial frontal craniotomy with the vascularized galeal flap (Fig. 1E). Cranioplasty is then performed for both craniotomies using bone flaps. Bone gaps are filled with bone chips and fibrin glue to avoid postoperative depression of the skull and face.

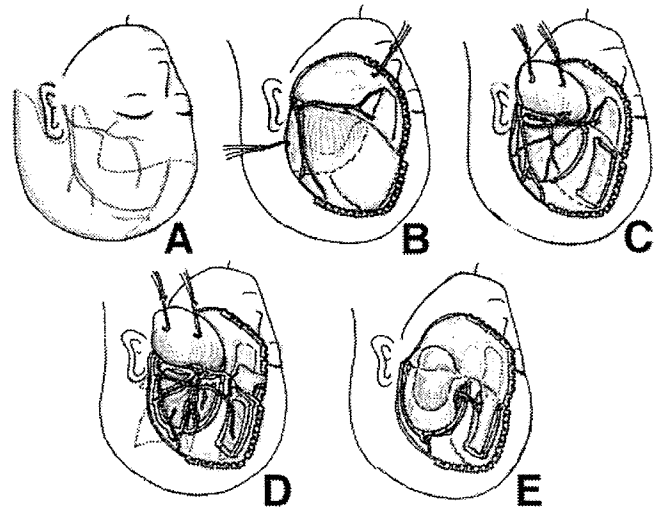

Fig. 1 Schematic drawings of the operative procedures. Skin incision is made along the course of the parietal branch of the superficial temporal artery (STA) and extended upward to the midline near the bregma and then along the midline downward to the hairline (A). Using this large skin flap, an adequate portion of the frontal branch of the STA can be dissected to reach the medial frontal area. The temporal muscle is separated as widely as possible. The galea of the frontal skin flap is also dissected, preserving a small vascular pedicle from the frontal branch of the STA (B). Two separate craniotomies are made, a frontotemporal craniotomy, which can be covered with the temporal muscle flap, and a medial frontal craniotomy, which can be covered with the galeal flap (C). The STA-anterior cerebral artery bypass and the STA-middle cerebral artery bypass are established (D). Encephalo-duro-arterio-myo-synangiosis is performed over the lateral craniotomy, and encephalo-galeo-arterio-synangiosis over the dural opening of the medial frontal craniotomy using the vascularized galeal flap (E).

Results

One pediatric patient suffered postoperative cerebral infarction in the frontal lobe manifesting as transient restless consciousness. Minor skin problems (localized alopecia along the skin incision) occurred although the STA branches were extensively separated from the scalp.

TIA completely disappeared in nine of the 11 patients presenting with TIA, and the frequency of TIA markedly reduced in the other two. Symptoms improved in all four patients presenting with cerebral infarction. Intellectual ability apparently improved in three of the four patients. Headache was attenuated in one of the two patients presenting with headache.

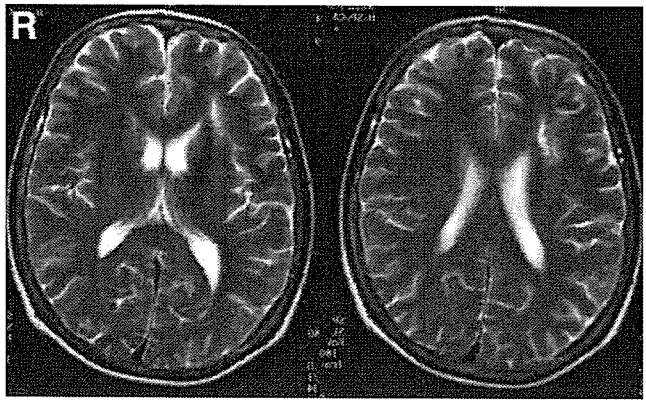

Fig. 2 Representative case of a 25-year-old woman (Case 9). T_2-weighted magnetic resonance images showing cerebral infarction in the subcortical area of the left frontal lobe.

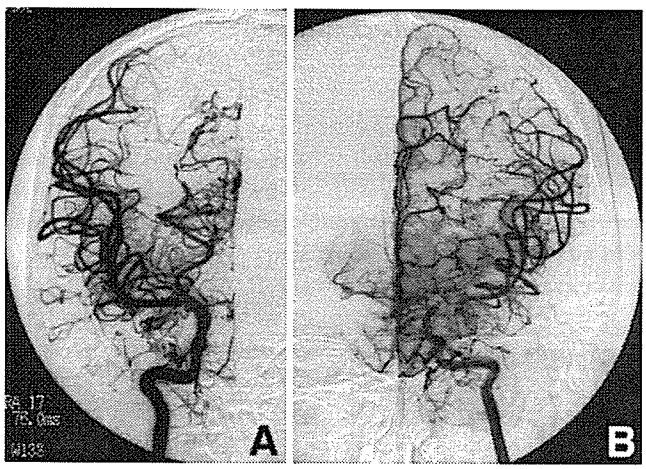

Fig. 3 Case 9. Right (A) and left (B) carotid angiograms, anteroposterior views, showing severe stenosis of the left internal carotid artery at the terminal portion associated with dilated moyamoya vessels, and mild stenosis of the right internal carotid artery and occlusion of the right anterior cerebral artery at the A_1 segment.

Illustrative Case Report

A 25-year-old woman (Case 9) visited our hospital complaining of dullness in the right upper extremity, emotional changes, and speech disturbance. Neurological examination found slight right hemiparesis and motor dominant aphasia. Magnetic resonance imaging showed cerebral infarction in the subcortical area of the left frontal lobe (Fig. 2). Cerebral angiography revealed severe stenosis of the left internal carotid artery at the terminal portion associated with dilated moyamoya vessels, and mild

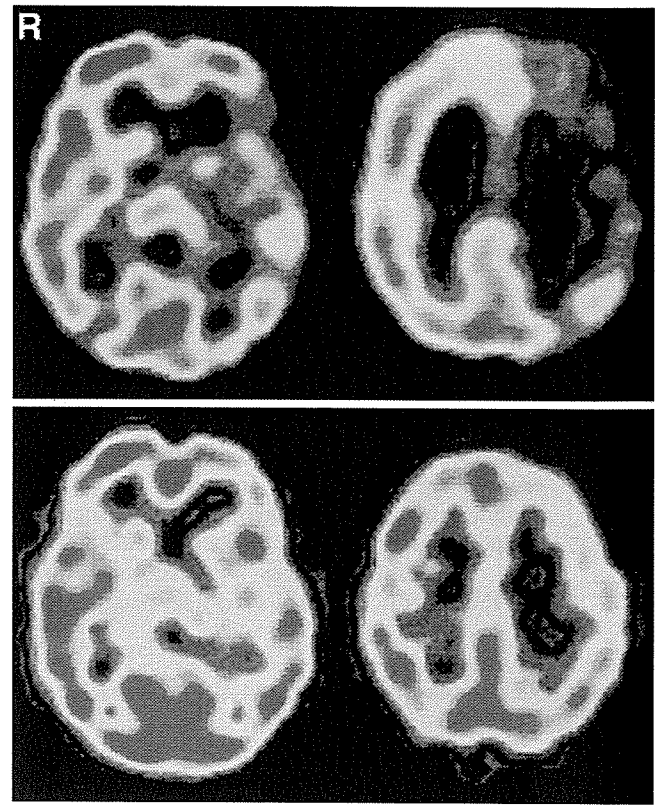

Fig. 4 Case 9. Preoperative (*upper row*) and postoperative (*lower row*) single photon emission computed tomography scans showing preoperative severe attenuation of the regional cerebral blood flow (rCBF) in both left anterior cerebral artery (ACA) and middle cerebral artery (MCA) territories, and postoperative markedly improved rCBF in both ACA and MCA territories.

stenosis of the right internal carotid artery and occlusion of the right ACA at the A_1 segment (Fig. 3). Single photon emission computed tomography (SPECT) showed severe attenuation of the regional CBF (rCBF) in both left ACA and MCA territories (Fig. 4 *upper row*).

She first underwent direct and indirect bypass surgery on the left. The proximal portion of the right ACA was occluded, so she also underwent the same procedure on the right 2 weeks after the first surgery. Postoperative course was uneventful. She completely recovered from the hemiparesis and aphasia. Postoperative left external carotid angiography 3 months after the surgery showed neovascularization from the direct and indirect bypasses (Fig. 5A). The stenosis of the right ACA was severe, but the STA-ACA bypass was patent and the STA was enlarged (Fig. 5B). The stenosis of the MCA was not so severe, so neovascularization in the

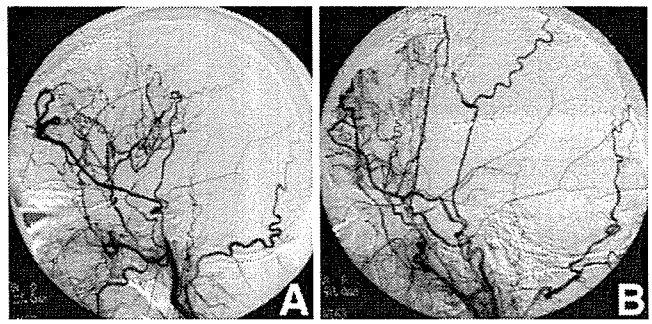

Fig. 5 Case 9. Left (A) and right (B) carotid angiograms, lateral views, taken at 3 months after vasoreconstructive surgery showing neovascularization from the direct and indirect bypasses on the left, and the patent superficial temporal artery (STA)-anterior cerebral artery bypass and enlarged STA on the right, but with less neovascularization in the middle cerebral artery territory.

MCA territory was not so rich at this time (Fig. 5B). Postoperative SPECT showed improved rCBF including the medial frontal area (Fig. 4 *lower row*). Her intellectual ability on the Wechsler Adult Intelligence Scale-Revised had increased from 66 in the preoperative period to 81 in the postoperative period. She returned to her previous job 4 months after the onset.

Discussion

TIAs in the lower extremities are known to persist after vasoreconstructive surgery in some patients. In particular, repetitive paraparetic TIA after the first operation (STA-MCA bypass and encephalomyo-synangiosis) was associated with poor cerebral hemodynamics in the frontal lobe in eight of 25 patients with pediatric moyamoya disease.[22] Various vasoreconstructive procedures for the frontal lobe have been performed. Direct STA-ACA bypass surgery was performed as a secondary surgery for refractory ischemic episodes.[5,7] Indirect bypass surgery targeting the frontal lobe,[21] ribbon EDAMS,[13] burr holes,[1,11] and dural pedicle insertion over the brain surface combined with encephalo-galeo-synangiosis[23] have also been reported. The present study describes the technical procedure to establish vasoreconstructive surgery including direct bypass for the ACA territory at the first intervention.

Known risk factors for perioperative ischemic complications include frequent TIAs, indirect bypass procedures, hemodynamic compromise, dehydration, lacrimation, hypotension, and hypercapnia as well as hypocapnia.[14] Blood flow directly supplied by the STA-ACA bypass, even if only a very small amount, may be helpful in preventing the perioperative risk of stroke and terminating postoperative ischemic symptoms, as found with STA-MCA bypass.[6] Indeed, we treated two patients who suffered infarction in the ACA territory after STA-MCA bypass combined with EDAMS.[15] We speculate that the blood supply to the ACA territory in those patients may have worsened with reduction of collateral flow through the moyamoya vessels as a result of changes in the hemodynamics after the STA-MCA bypass combined with EDAMS.[14] Avoiding the risk of hypoperfusion in the ACA territory is also important in the perioperative period for improving the outcome, especially if the patient has impaired preoperative hemodynamics in the ACA territory. On the other hand, if the ischemia is located only in the MCA territory, we should anastomose pedicles of the STA mainly to branches of the MCA.

Vasoreconstructive surgery through "small craniotomy" does not improve cerebral hemodynamics in the frontal lobe.[14,18,22] Intellectual outcome is an important consideration in treating patients with moyamoya disease.[10] Recent studies have suggested a close relationship between intellectual development and frontal lobe function in children.[2] Chronic blood flow reduction in the frontal lobe may be responsible for poor intellectual outcome. Ischemic attacks were still observed after a mean of 6 years 11 months in half of a series of the TIA-type patients treated nonsurgically, whereas the ischemic symptoms disappeared within 5 years after onset in the other half.[3] The TIA-type patients had a good intellectual prognosis.[3] Other studies have suggested that intellectual impairment would progress, even in TIA-type patients, if they did not undergo appropriate surgical treatment.[16,19] We are not certain whether direct STA-ACA bypass is always necessary or only indirect bypass targeting the medial frontal area such as EGAS is sufficient for this intellectual improvement. Further follow-up studies are necessary.

In conclusion, simultaneous STA-MCA and STA-ACA bypasses with pan-synangiosis are suitable for patients with moyamoya disease associated with severely impaired perfusion in the ACA territory requiring direct bypass surgery. The surgical procedure may prevent intellectual deterioration and improve the overall outcome by normalizing cerebral hemodynamics in the frontal lobe.

References

1) Endo M, Kawano N, Miyasaka Y, Yada K: Cranial burr hole for revascularization in moyamoya disease. *J Neurosurg* 71: 180-185, 1989
2) Filley CM: Clinical neurology and executive dysfunction. *Semin Speech Lang* 21: 95-108, 2000
3) Fukuyama Y, Umezu R: Clinical and cerebral angiographic evaluations of idiopathic progressive occlusive disease of the circle of Willis ('moyamoya' disease) in children. *Brain Dev* 7: 21-37, 1985
4) Houkin K, Kamiyama H, Takahashi A, Kuroda S, Abe H: Combined revascularization surgery for childhood moyamoya disease: STA-MCA and encephalo-duro-arterio-myo-synangiosis. *Childs Nerv Syst* 13: 24-29, 1997
5) Ishii R, Koike T, Takeuchi S, Ohsugi S, Tanaka R, Konno K: Anastomosis of the superficial temporal artery to the distal anterior cerebral artery with interposed cephalic vein graft. Case report. *J Neurosurg* 58: 425-429, 1983
6) Ishikawa T, Houkin K, Kamiyama H, Abe H: Effects of surgical revascularization on outcome of patients with pediatric moyamoya disease. *Stroke* 28: 1170-1173, 1997
7) Iwama T, Hashimoto N, Miyake H, Yonekawa Y: Direct revascularization to the anterior cerebral artery territory in patients with moyamoya disease: report of five cases. *Neurosurgery* 42: 1157-1162, 1998
8) Karasawa J, Kikuchi H, Furuse S, Kawamura J, Sakai T: Treatment of moyamoya disease with STA-MCA anastomosis. *J Neurosurg* 49: 679-688, 1978
9) Karasawa J, Kikuchi H, Kawamura J, Sakai T: Intracranial transplantation of the omentum for cerebrovascular moyamoya disease. *Surg Neurol* 32: 527-531, 1993
10) Karasawa J, Touho H, Ohnishi H, Miyamoto S, Kikuchi H: Long-term follow-up study after extracranial-intracranial bypass surgery for anterior circulation ischemia in childhood moyamoya disease. *J Neurosurg* 77: 84-89, 1992
11) Kawaguchi T, Fujita S, Hosoda K, Shose Y, Hamano S, Iwakura M, Tamaki N: Multiple burr-hole operation for adult moyamoya disease. *J Neurosurg* 84: 468-476, 1996
12) Kinugasa K, Mandai S, Kamata I, Sugiu K, Ohmoto T: Surgical treatment of moyamoya disease: operative technique for encephalo-duro-arterio-myo-synangiosis, its follow-up, clinical results, and angiograms. *Neurosurgery* 32: 527-531, 1993
13) Kinugasa K, Mandai S, Tokunaga K, Kamata I, Sugiu K, Handa A, Ohmoto T: Ribbon encephalo-duro-arterio-myo-synangiosis for moyamoya disease. *Surg Neurol* 41: 455-461, 1994
14) Kuroda S, Houkin K, Ishikawa T, Nakayama N, Ikeda J, Ishii N, Kamiyama H, Iwasaki Y: Determinants of intellectual outcome after surgical revascularization in pediatric moyamoya disease: a multivariate analysis. *Childs Nerv Syst* 20: 302-308, 2004
15) Kuroda S, Houkin K, Nunomura M, Abe H: Frontal lobe infarction due to hemodynamic change after surgical revascularization in moyamoya disease — two case reports. *Neurol Med Chir (Tokyo)* 40: 315-320, 2000
16) Kurokawa T, Tomita S, Ueda K, Narazaki O, Hanai T, Hasuo K, Matsushima T, Kitamura K: Prognosis of occlusive disease of the circle of Willis (moyamoya disease) in children. *Pediatr Neurol* 1: 274-277, 1985
17) Matsushima T, Fujiwara S, Nagata S, Fujii K, Fukui K, Hasuo K: Reoperation for moyamoya disease refractory to encephalo-duro-arterio-synangiosis. *Acta Neurochir (Wien)* 107: 129-132, 1990
18) Matsushima T, Inoue T, Suzuki SO, Fujii K, Inoue T, Fukui M, Hasuo K: Surgical treatment of moyamoya disease in pediatric patients — comparison between the results of indirect and direct revascularization techniques. *Neurosurgery* 31: 401-405, 1992
19) Matsushima Y, Aoyagi M, Koumo Y, Takasato Y, Yamaguchi T, Masaoka H, Suzuki R, Ohno K: Effects of encephalo-duro-arterio-synangiosis on childhood moyamoya patients — swift disappearance of ischemic attacks and maintenance of mental capacity. *Neurol Med Chir (Tokyo)* 31: 708-714, 1991
20) Matsushima Y, Aoyagi M, Masaoka H, Suzuki R, Ohno K: Mental outcome following encephaloduroarteriosynangiosis in children with moyamoya disease with the onset earlier than 5 years of age. *Childs Nerv Syst* 6: 440-443, 1990
21) Suzuki Y, Negoro M, Shibuya M, Yoshida J, Negoro T, Watanabe K: Surgical treatment for pediatric moyamoya disease: Use of the superficial temporal artery for both areas supplied by the anterior and middle cerebral arteries. *Neurosurgery* 40: 324-330, 1997
22) Touho H, Karasawa J, Ohnishi H: Preoperative and postoperative evaluation of cerebral perfusion and vasodilatory capacity with 99mTc-HMPAO SPECT and acetazolamide in childhood Moyamoya disease. *Stroke* 27: 282-289, 1996
23) Yoshida YK, Shirane R, Yoshimoto T: Non-anastomotic bypass surgery for childhood moyamoya disease using dural pedicle insertion over the brain surface combined with encephalogaleomyosynangiosis. *Surg Neurol* 51: 404-411, 1999

Address reprint requests to: T. Ishikawa, M.D., Department of Neurosurgery, Saitama Medical Center, 1981 Kamoda, Kawagoe, Saitama 350-8550, Japan.

Commentary

Ishikawa and colleagues are congratulated on fantastic outcomes in 16 cases where unilateral (n = 6) or bilateral (n = 10) extensive combined direct and indirect ACA and MCA revascularization was performed for moyamoya disease. The procedure is well described, including low flow (direct STA to MCA and STA to ACA) bypass and indirect encephalo-duro-arterio-myo-synangiosis and encephalo-galeo-arterio-synangiosis for MCA and ACA territories, respectively. Cases included eight pediatric (as young as 5 years of age) and eight adult patients. There was only one reported minor infarct and no other complications in the 26 procedures. This alone is a technical feat, and the results are surely compelling.

The authors attribute their superior results to the comprehensive revascularization strategy, where more conservative operations, especially the lack of STA-ACA direct bypass, would leave patients vulnerable to immediate perioperative risks in that territory. However, that is not necessarily a consistent proposition. Reported complications of surgery for moyamoya disease in the published literature and in anecdotal experience are not always related to the ACA territory. And there were apparently no complications related to staging second hemisphere revascularization in cases where the authors felt it was needed. The authors tell us that they managed 35 hemispheres in 22 patients with moyamoya disease during the same period, hence the majority of cases received the extensive procedure. And they state that they did not carry out planned ACA direct anastomosis in some cases for technical reasons. But the authors do not report results of intention to treat decision, where such strategy was attempted and could not be carried out (in up to 6 patients and 9 hemispheres), and what was the outcome of those cases.

The authors attempt to articulate specific indications for this aggressive procedure, but they apparently ultimately performed it on the majority of moyamoya cases in their series, and they admit that they attempted it in even more patients. Hence we are left at loss as to when such aggressive strategy would NOT be justified... Nevertheless, the authors do demonstrate apparent feasibility and safety of this very elegant operation in their patients and in their hands. We would caution against generalization to cases of moyamoya syndrome in other experience, including adult patients outside Japan, where basal occlusive vasculopathy may have different etiologies, and disease course, and where scalp vessel may not allow direct ACA anastomosis in most instances. And we must await confirmation of similar feasibility and safety when this approach is attempted on similar patients by other surgeons.

Issam A. AWAD, M.D., M.Sc., F.A.C.S., M.A. (Hon.)
Evanston Northwestern Healthcare
Department of Neurological Surgery
Northwestern University
Feinberg School of Medicine
Evanston, Illinois, U.S.A.

This interesting paper raises several important points, among them that improving flow in one area may alter the hemodynamics enough to cause more severe ischemia in an adjacent area with previous borderline flow. The anterior cerebral artery territory tends to be neglected in ordinary ischemic situations but is obviously more at risk in moyamoya disease where the vascular changes are so widespread. The authors have obviously a lot of experience with this condition, and have suggested useful additions to the usual bypass procedures.

Another important point, raised in their discussion, is the significance of frontal lobe blood flow and function in children versus adults. The developing brain may well be more vulnerable to ischemia at this stage, particularly from the point of view of future intellectual performance. However, it is equally interesting that two of the patients with measured improvement in IQ were adults (Table 1); frontal lobe impairment to the extent seen here is probably important at any age.

Nicholas W. C. DORSCH, M.D., F.R.C.S., F.R.A.C.S.
Department of Neurosurgery
Westmead Hospital
Sydney, Australia

The conventional and routine surgical technique for moyamoya disease covers mostly the middle cerebral artery territory by STA-MCA direct bypass and encephalosynangiosis using the temporal muscle. In other words, revascularization to the anterior cerebral artery territory is not always satisfactory using the conventional surgical technique including direct and indirect bypass surgery.

In this paper, Ishikawa et al. have reported an excellent technique to overcome these drawbacks. They have aggressively performed STA-ACA direct bypass for patients with moyamoya disease and its outcome is excellent. This is a quite unique and enthusiastic challenge.

However, this technique is quite intricate and not always accepted as a general option for this disease. There are some questions raised by this paper. Among them, the indication of this technique is quite controversial. It is obvious that this surgery takes more time and seems to be more invasive compared to the other conventional techniques. In my personal series, transient ischemic attack due to ischemia of the anterior cerebral artery territory is not always permanent after successful revascularization surgery even using the conventional techniques. It seems, therefore, the indication of this complicated surgery seems to be narrower than described in this paper.

I believe that this technique is theoretically acceptable for very limited cases of moyamoya disease. However, it has to be emphasized that this technique requires a superb background in fine microsurgical vascular anastomosis technique and considerable experience in the treatment of moyamoya disease.

Kiyohiro HOUKIN, M.D.
Department of Neurosurgery
Sapporo Medical University
Sapporo, Hokkaido, Japan

Journal of Neuroscience Research 84:1187–1196 (2006)

Bcl2 Enhances Survival of Newborn Neurons in the Normal and Ischemic Hippocampus

Tsutomu Sasaki,[1]* Kazuo Kitagawa,[1] Yoshiki Yagita,[1] Shiro Sugiura,[1] Emi Omura-Matsuoka,[1] Shigeru Tanaka,[1] Kohji Matsushita,[1] Hideyuki Okano,[3] Yoshihide Tsujimoto,[2] and Masatsugu Hori[1]

[1]Division of Stroke Research, Department of Cardiovascular Medicine, Osaka University Graduate School of Medicine, Osaka, Japan
[2]Division of Molecular Genetics, Department of Post-Genomics and Diseases, Osaka University Graduate School of Medicine, Osaka, Japan
[3]Department of Physiology, Keio University Graduate School of Medicine, Shinjyuku-ku, Tokyo, Japan

Neuronal progenitors in the adult hippocampus continually proliferate and differentiate to the neuronal lineage, and ischemic insult promotes hippocampal neurogenesis. However, newborn neurons show a progressive reduction in numbers during the initial few weeks, therefore, enhanced survival of newborn neurons seems to be essential for therapeutic strategy. Bcl-2 is a crucial regulator of programmed cell death in CNS development and in apoptotic and necrotic cell death. Therefore, we tested whether Bcl-2 overexpression enhances survival of newborn neurons in the adult mouse hippocampus under normal and ischemic conditions. Many newborn neurons in the hippocampal dentate gyrus undergo apoptosis. Human Bcl-2 expression in NSE-bcl-2 transgenic mice began at the immature neuronal stage and remained constant in surviving mature neurons. Bcl-2 significantly increased survival of newborn neurons under both conditions, but particularly after ischemia, with decreased cell death of newborn neurons in NSE-bcl-2 transgenic mice. We also clarified the effect by Bcl-2 overexpression of enhanced survival of newborn neurons in primary hippocampal cultures with BrdU labeling. These findings suggest that Bcl-2 plays a crucial role in adult hippocampal neurogenesis under normal and ischemic conditions.

Key words: Bcl-2; hippocampus; neurogenesis; ischemia

In adult hippocampal neurogenesis, nascent neurons show a progressive reduction (Kempermann et al., 2003), and surviving neurons became integrated into the dentate granule cell circuitry (van Praag et al., 2002). Continued production of hippocampal granule cells is combined with elimination of cells via spontaneous apoptosis, with turnover occurring throughout life (Gould and Cameron, 1996; Young et al., 1999). Running exercise and enriched environment promote the survival of newborn neurons (van Praag et al., 1999; Young et al., 1999). Thus, enhanced survival of newborn neurons seems beneficial.

Brain ischemia enhances neurogenesis in the hippocampus (Liu et al., 1998; Yagita et al., 2001) and also induces migration of neuroblasts into lesions in nonneurogenic areas such as the striatum (Arvidsson et al., 2002). However, only a small fraction of these newborn neurons survive (Liu et al., 1998; Yagita et al., 2001; Arvidsson et al., 2002). Despite accumulating data on the mechanisms responsible for neuronal progenitor proliferation after ischemia, little is understood regarding the signals that control survival of newborn neuron after ischemia. Bcl-2 levels were increased in the hippocampus after ischemia (Chen et al., 1997). Bcl-2 has been shown to be protective against apoptotic and necrotic cell death in response to various stimuli, including exposure to glutamate or ischemia (Martinou et al., 1994; Adams and Cory, 1998; Kitagawa et al., 1998). Moreover, neurotrophins play a crucial role in adult neurogenesis following ischemia as well as under normal conditions (Pencea et al., 2001). Bcl-2 has been reported to mediate the survival effects of neurotrophins such as BDNF and NGF. Based on these findings, it is essential to examine the effect of Bcl-2 on the survival of newborn neurons after ischemia.

During central nervous system (CNS) development, BCL-2 has been shown to be a key regulator of programmed cell death (Abe-Dohmae et al., 1993; Martinou et al., 1994). Programmed cell death has often been found in regions in which neurogenesis persists throughout adulthood, including the hippocampus and olfactory bulb.

Contract grant sponsor: Japan Society for the Promotion of Science; Contract grant sponsor: Takeda Science Foundation.

*Correspondence to: Tsutomu Sasaki, Division of Stroke Research, Department of Cardiovascular Medicine, Osaka University Graduate School of Medicine, 2-2 Yamadaoka, Suita City, Osaka 565-0871, Japan. E-mail: sasaki@medone.med.osaka-u.ac.jp

Received 3 April 2006; Revised 29 June 2006; Accepted 30 June 2006

Published online 29 August 2006 in Wiley InterScience (www.interscience.wiley.com). DOI: 10.1002/jnr.21036

We sought to determine whether overexpression of the human *bcl-2* transgene increases survival of newborn neurons in the hippocampal dentate gyrus under normal and ischemic conditions.

MATERIALS AND METHODS

Animals

All research was conducted according to a protocol approved by the Institutional Animal Care and Use Committee of Osaka University Graduate School of Medicine. Adult 11- to 12-weeks-old male C57Black/6 mice and transgenic mice overexpressing BCL-2 under a neuron-specific enolase promoter (NSE-*bcl-2* transgenic mice) (Martinou et al., 1994) were used. NSE-*bcl-2* transgenic mice were backcrossed to C57Black/6 mice 10 times. The genotype was confirmed postmortem by PCR amplification of tail genomic DNA. The amount of Bcl-2 expression in wild-type and NSE-*bcl-2* transgenic mice were evaluated by Western blotting.

Bromodeoxyuridine Labeling Protocols and Immunohistochemistry

To quantify and evaluate the phenotype of newborn cells, bromodeoxyuridine (BrdU; Roche Diagnostics, Indianapolis, IN) was given four times every 2 hr during a period of 6 hr. At 1, 7, 14, 21, and 30 days after BrdU administration, mice were sacrificed under deep pentobarbital anesthesia and transcardially perfused with 4% paraformaldehyde (PFA). Brains were removed and fixed in 4% PFA at 4°C.

Next, we used NSE-*bcl-2* transgenic mice including wild-type mice. BrdU-labeling protocols and the processing were the same above. To examine the proliferation of newborn neurons in the SGZ in both groups, mice were sacrificed 1 day after BrdU administration. To evaluate the survival or differentiation of newborn neurons, mice were decapitated 30 days after BrdU administration.

Each tissue block was embedded in paraffins. The protocol of BrdU immunohistochemistry was described previously (Sasaki et al., 2003). Sections were treated in 50% formamide and 2× SSC and then incubated in 2N HCl. Sections were incubated with a rat monoclonal anti-BrdU antibody, 1 : 100 (Harlan Sera-Labo, Loughborough, UK) at 4°C overnight. Sections were then incubated with a biotinylated secondary antibody, and further incubated with a streptavidin–biotin–peroxidase complex (Vector Laboratories, Burlingame, CA). To count BrdU-positive cells, five sections from the hippocampus were cut every 120 μm beginning 1.4 mm caudal and 1.9 mm caudal to the bregma. In the hippocampus, the granular cell layer (GCL) and SGZ, defined as a zone two cell bodies wide along the border of the GCL and hilus, were considered together for quantification. The mean density of BrdU-positive cells in each mouse was calculated as the number of labeled nuclei divided by the area.

For double-immunofluorescence, 40 μm-thick free-floating sections were incubated with primary antibody at 4°C overnight. The following primary antibodies were used: a monoclonal antibody against human BCL-2 (Dakocytomation, Denmark A/S), a rat monoclonal anti-BrdU antibody, 1 : 100 (Harlan Sera-Labo, Loughborough, UK), mouse monoclonal anti-BrdU antibody, 1 : 200 (Amersham, Piscataway, NJ), mouse monoclonal anti-NeuN antibody, 1:200 (Chemicon, Temecula, CA), rabbit polyclonal anti-glial fibrillary acidic protein (GFAP) antibody, 1 : 200 (Sigma), goat polyclonal anti-double cortin (DCX) antibody, 1 : 100 (Santa Cruz Biotechnology, Santa Cruz, CA), rat monoclonal anti-Musashi-1 (Msi-1) antibody (14H1) 1 : 200, mouse monoclonal anti-β-tubulin III antibody, 1 : 200 (Chemicon) mouse monoclonal PSA-NCAM, 1:200 (Pharmingen, San Jose, CA), and mouse monoclonal anti human BCL-2 antibody (Dako, 1 : 200). Sections were incubated with appropriate secondary donkey antibodies conjugated to FITC or rhodamine (Chemicon, 1 : 200) for 90 min at room temperature, and visualized or photographed with a confocal microscopy system (Zeiss LSM-510).

TUNEL Staining

To identify cells apoptosis, TUNEL labeling was carried out. Brain was removed rapidly en bloc and quickly frozen in liquid N_2 vapor. Sections 14 μm thick were cut on a cryostat and post-fixed in 1% PFA for 10 min. The Apoptag Fluorescein In Situ Apoptosis Detection Kit (S7110; Chemicon) was then applied. For immuno fluorescein-double labeling of TUNEL signal and BrdU, the TUNEL-fluorescein labeling was carried out first, followed by incubation in 2N HCl for 30 min at 37°C, and application of a rat monoclonal anti-BrdU antibody.

Transient Forebrain Ischemia

General anesthesia was maintained with 1% halothane. A column for measurement of cortical microperfusion by Laser-Doppler flowmetry (advanced laser flowmetry) was attached to the skull. Body and skull temperature were monitored and maintained at 36.5°C to 37.5°C. Both common carotid arteries were occluded for 12 min with microaneurysm clips and then reperfused. As described previously, only mice that showed <13% of baseline control microperfusion during the first minute of occlusion were used (Kitagawa et al., 1998). To examine the profiles of newborn neurons after ischemia, we injected BrdU (50 mg/kg, i.p.) 9 days after ischemia reported previously (Sasaki et al., 2003). As in normal conditions, BrdU was given four times every 2 hr. Thereafter, mice subjected to ischemia were processed under the same schedule as normal condition (each time-point 1, 4, 7, 14, and 30 days after BrdU administration).

Western Blotting

Samples of the hippocampus and the cortex of both NSE-bcl-2 transgenic mice and wild-type littermates were isolated. Proteins were separated by SDS-PAGE and transferred electrophoretically to polyvinylidene difluoride sheet (Immunobilon P; Millipore, Bedford, MA). Blots were probed with a mouse monoclonal bcl-2 antibody (Santa Cruz Biotechnology; 1 : 1,000), and a mouse monoclonal human bcl-2 antibody (Dakocytomation; 1 : 1,000), then detected using sheep anti-mouse HRP-conjugated secondary antibody (Amersham Pharmacia Biotech, Buckinghamshire, UK) followed by enhanced chemoluminescence (ECL; Amersham Pharmacia Biotech).

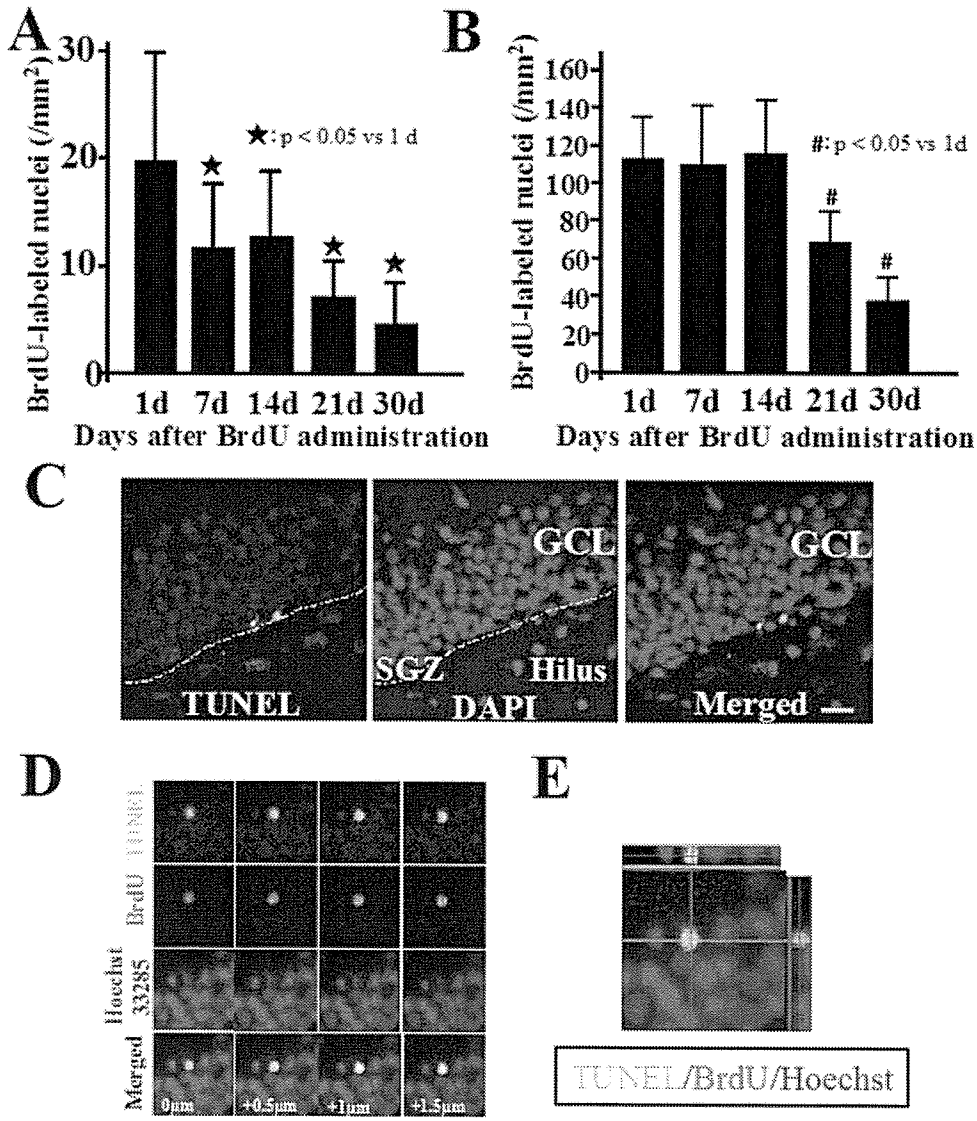

Fig. 1. Temporal profiles of BrdU-positive cells in normal (**A**) and ischemia (**B**) (n = 6). $^{\#,\star}P < 0.05$ vs. 1 day. **C:** TUNEL staining under normal condition in the dentate gyrus. Scale bar = 20 μm. **D,E:** At 21 days after BrdU administration, some of BrdU-positive cells showed TUNEL-positive, with the blue nuclear counterstain Hoechst 33258. Higher magnification views of selected individual z-planes (D) and a Z-series through the section (Z-distance = 10 μm) (E).

Neuron–Glia Mixed Cultures

To evaluate the direct effect of Bcl-2 on survival of newborn hippocampal neurons, primary hippocampal cultures from NSE-bcl-2 transgenic mice and their littermates were analyzed as described previously (Fujioka et al., 2004). The production of most hippocampal neuron is completed before birth in the mouse (between E15–E17), however, 85% of the hippocampal granular neurons in the dentate gyrus are generated postnatally (Bayer, 1980). It is widely known that granular neurons in the dentate gyrus show turnover throughout adulthood. Based on these findings, to directly confirm the findings that overexpression of BCL-2 enhanced the survival of nascent neurons in vivo, we carried out primary hippocampal culture with BrdU labeling at P0. To identify newborn neurons, BrdU (100 mg/kg, i.p.) was administered to P0 neonatal mice twice over 2 hr, and the hippocampus were dissected on P1 into HBSS without calcium or magnesium. Cells were dissociated with 1% trypsin (Invitrogen) and plated onto 6-cm dishes coated with Matrigel (BD Biosciences). Cells at a final concentration of 5×10^5 cells/ml were cultured in high-glucose DMEM (Sigma) containing 10% fetal calf serum. Twelve hours after seeding, the medium was changed to neuro basal medium supplemented with B-27 (Life Technologies), L-glutamine, 100 IU/ml penicillin, and 100 μg/ml streptomycin. Cells were cultured at 37°C in a humidified atmosphere of 95% air and 5% CO_2. These cultures contained neurons and astrocytes. After 13–15 days, the neurons in these cultures sit on the top of a confluent monolayer of astrocytes. At 1, 7, 14, and 30 days after seeding, cells were fixed immediately with 4% PFA for 30 min. Cells were then incubated with primary antibody at 4°C overnight. The slides were washed in three changes of phosphate-buffered saline, incubated with appropriate secondary donkey antibodies conjugated to FITC or rhodamine (Chemicon, 1 : 200) for 90 min at room temperature, and visualized or photographed with a confocal microscopy system (Zeiss LSM-510). The number of Tuj-1-positive neurons and Tuj-1/BrdU double-positive cells was counted in a field of 1 cm^2.

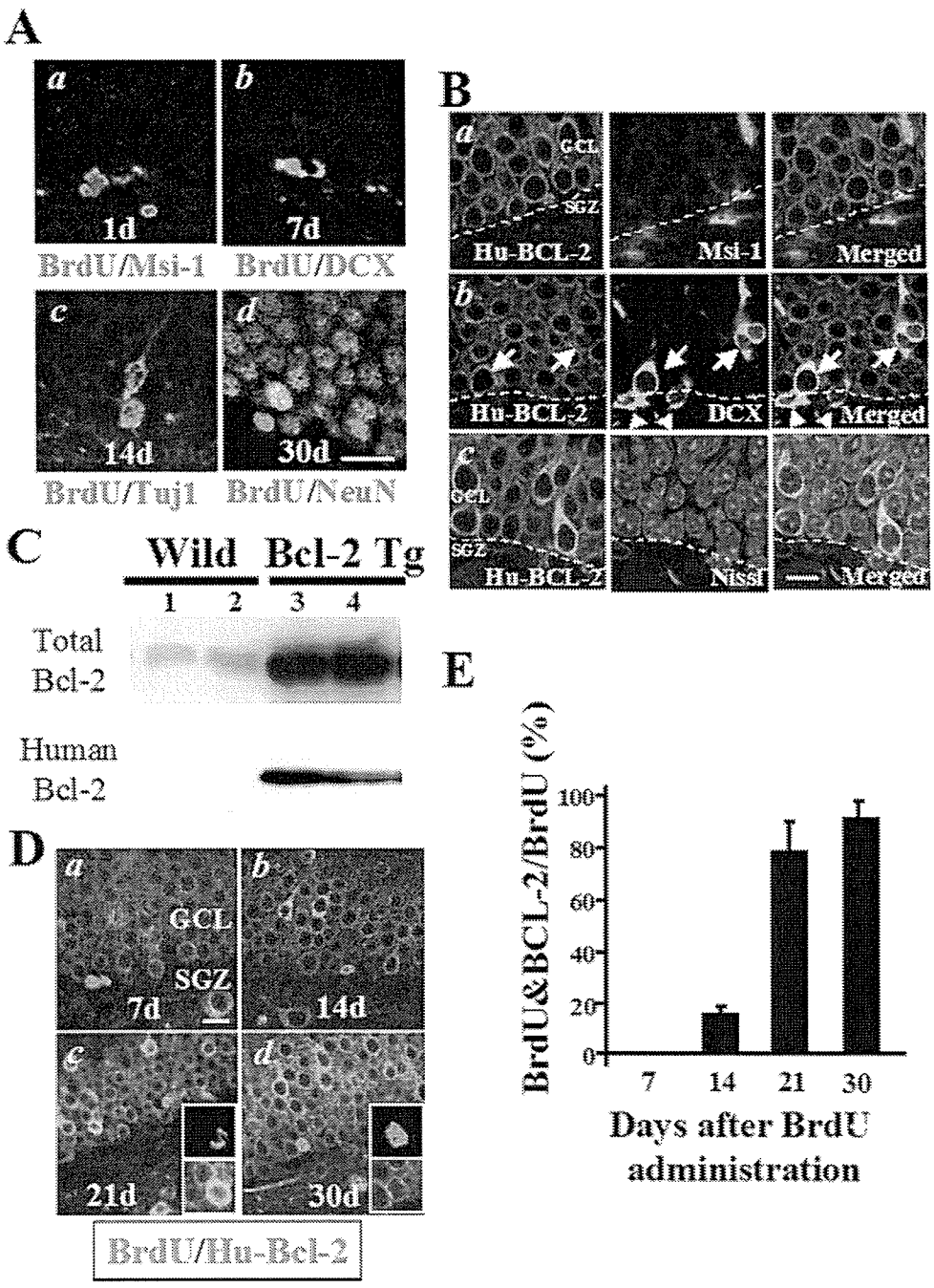

Fig. 2. **A:** Double-immunofluorescence staining of BrdU/Msi-1, BrdU/DCX, BrdU/Tuj1, and BrdU/NeuN was carried out. **B:** Expression of human Bcl-2 in NSE-*bcl-2* transgenic mice. **C:** Western blots analysis of total Bcl-2 and Human Bcl-2. Lane 1, hippocampus; lane 2, cortex ; lane 3, hippocampus; lane 4, cortex. **D,E:** Time course of human Bcl-2 immunoreactivity in BrdU-positive newborn neurons. Right insets in (C) show confocal images for BrdU (red) and Bcl-2 (green) from NSE-*bcl-2* transgenic mice (D) (n = 5). Scale bar = 20 μm (A), 10 μm (B), 30 μm (D).

Statistics

Data in the text and figures were described mean ± SD. Multiple comparisons were evaluated statistically by the analysis of variance, followed by Scheffé's post-hoc tests.

RESULTS

Survival of Newborn Cells in the Dentate Gyrus Under Normal and Ischemic Conditions

We determined the number of BrdU-positive cells and the phenotype of postmitotic cells at 1, 7, 14, 21, and 30 days after BrdU administration. Under normal conditions, the number of BrdU-positive cells showed a progressive reduction (1, 7, 14, 21, and 30 days; 19.7 ± 10.9, 11.3 ± 6.8, 12.3 ± 8.4, 8.7 ± 4.3, 4.8 ± 4.6/mm^2, respectively) (Fig. 1A). Next, we used double-immunolabeling with BrdU antibody and Msi-1 for neuronal progenitors, DCX for migrating neuroblast and immature neurons, Tuj1 for immature neurons, or NeuN for mature neurons (Fig. 2A). Most BrdU-positive cells in the SGZ showed Msi-1 staining 1 day after BrdU administration (Fig. 2Aa). Staining for DCX in BrdU-positive cells

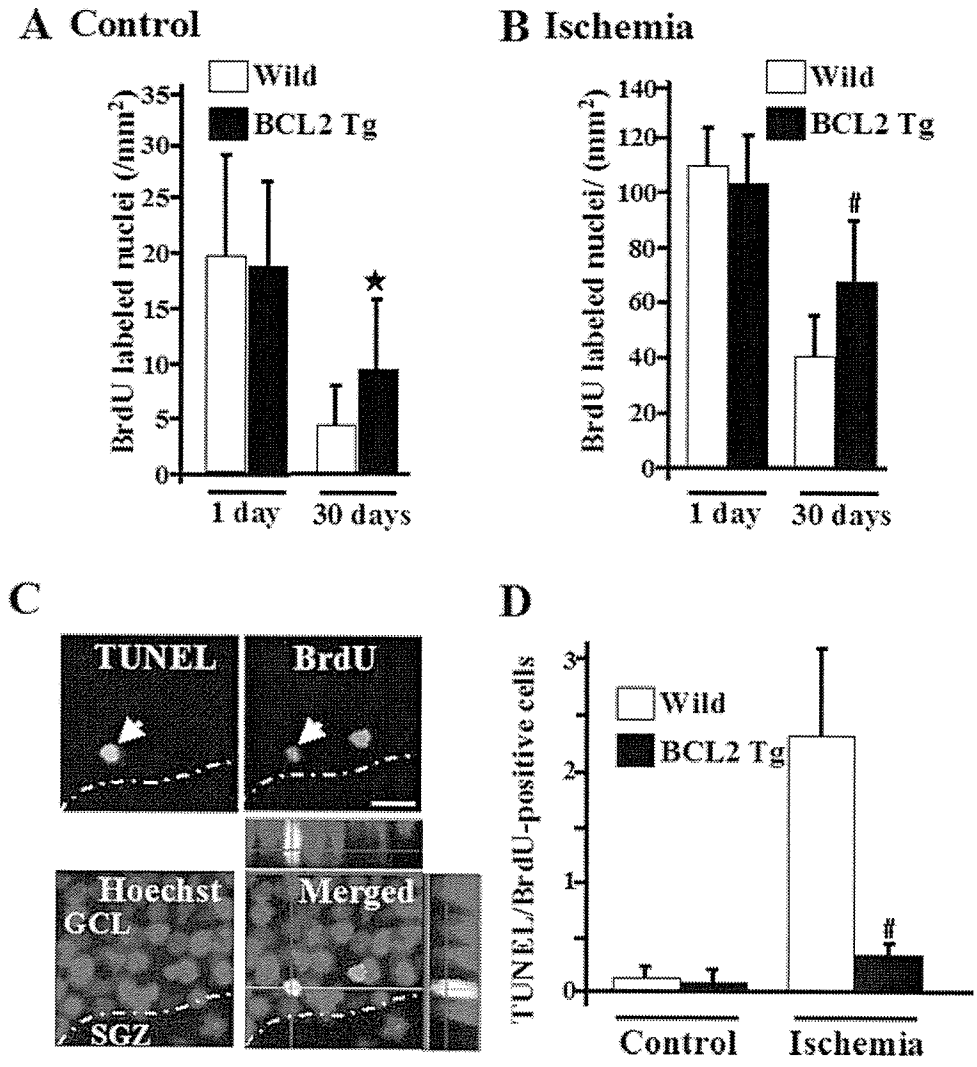

Fig. 3. Bcl-2 overexpression enhanced survival of hippocampal newborn neurons under normal (**A**) (n = 7) and ischemic conditions (**B**) (n = 8). **C,D:** Colocalization of TUNEL staining and BrdU after ischemia was shown (C, arrow), (Z-distance is 20 μm). Scale bar = 20 μm. **D:** Quantification of apoptosis of newborn neurons under normal and ischemic conditions. The number of BrdU/TUNEL double-positive cells at 21 days after BrdU administration was counted (n = 10). $^{\#}P < 0.05$ vs. normal.

peaked at 7–14 days, but declined dramatically 30 days after BrdU injection. BrdU-positive cells showing DCX or Tuj1 staining over time were similar (Fig. 2Ab,c). In contrast, BrdU/NeuN double-positive cells in the GCL were rare at 14 days after BrdU administration, and increased thereafter, and the majority of BrdU-positive cells showed NeuN staining at 30 days (Fig. 2Ad). The switch from expression of DCX or Tuj1 to NeuN seemed to occur between 14–30 days. Under ischemic conditions, there was no significant difference between the number of cells at 1 day and 14 days, thereafter, the numbers of BrdU-positive cells gradually declined up to 30 days (1, 7, 14, 21, and 30 days; 115.5 ± 23.7, 114.5 ± 30.5, 120.9 ± 32.9, 68.2 ± 13.0, and 38.7 ± 13.1/mm^2; Fig. 1B). To evaluate the contribution of apoptotic cell death to the progressive reduction in newborn cells, we used double-immunolabeling with anti-BrdU antibody and TUNEL staining. TUNEL-positive cells were detected in the SGZ and the inner layer of the GCL (Fig. 1C). Some of TUNEL-positive cells were also BrdU-positive at 21 days after BrdU administration (Fig. 1D,E).

Expression of the Human Bcl-2 Transgene During Adult Hippocampal Neurogenesis

Western blot analysis showed that the amount of total bcl-2 protein including both endogenous mouse bcl-2 and transgene human bcl-2 in NSE-*bcl-2* transgenic mice was augmented significantly compared to that in wild-type. Human bcl-2 protein was detected only in NSE-*bcl-2* transgenic mice (Fig. 2C). Double-immunolabeling with the antibody that recognized only human bcl-2 was carried out (Fig. 2B,D,E). To examine the expression of human Bcl-2 in NSE-*bcl-2* transgenic mice, double-immunofluorescence was carried out (Fig. 2B). Msi-1-positive cells in the SGZ did not stain for Bcl-2 (Fig. 2Ba). DCX- positive cells in the SGZ did not show immunostaining for Bcl-2 (Fig. 2Bb, arrowheads). In contrast, immature neurons within the GCL, as they migrated from the inner toward the outer layer, showed colocalization of DCX and Bcl-2 (Fig. 2Bb, arrows). Most Nissl-positive mature neurons showed Bcl-2 staining (Fig 2Bc). Expression of the transgene was rarely detected as early as 14 days after BrdU administration, but increased in number thereafter and

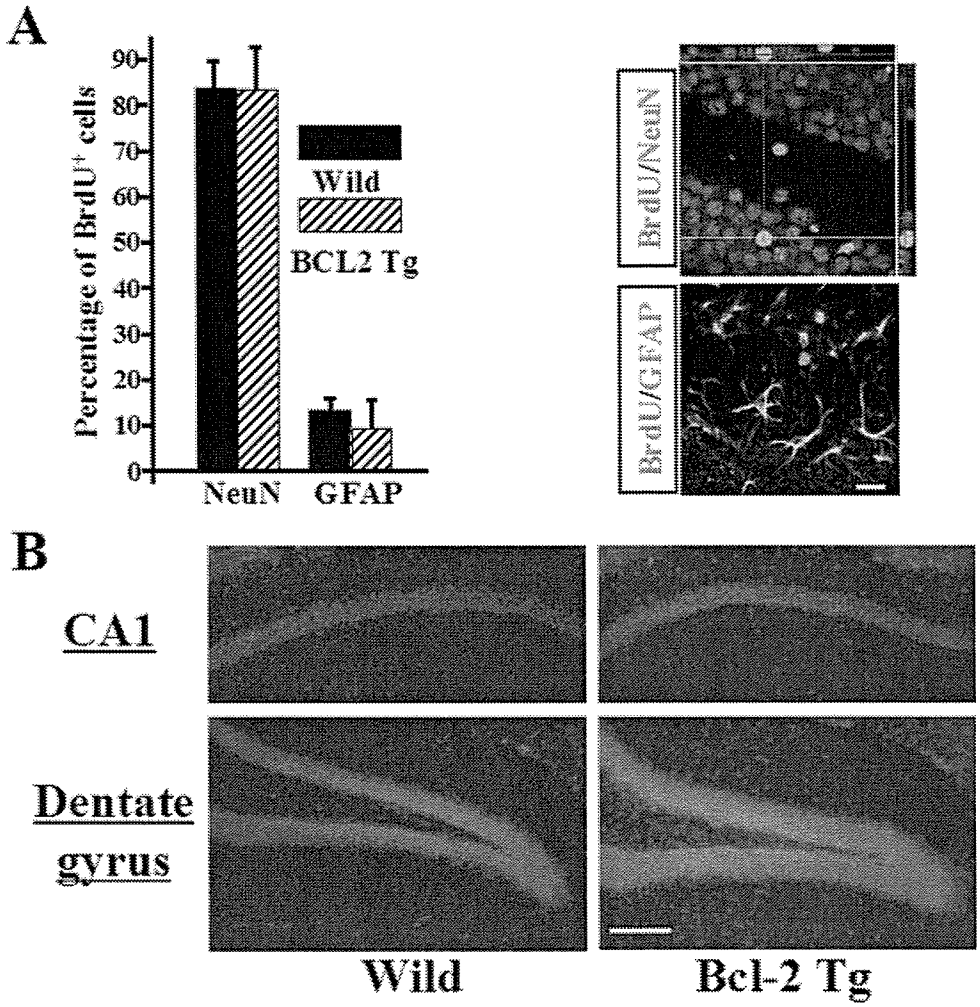

Fig. 4. **A:** We examined the effect of bcl-2 overexpression on the differentiation of newborn neurons. **B:** Total volume of cells in the hippocampal CA1 sector (upper panel) or in the dentate gyrus (lower panel) of NSE-*bcl-2* transgenic mice and wild-type littermates in the 18-month-old mouse. Scale bar = 30 μm (B), 100 μm (C).

became stable (Fig. 2Da–d). Semiquantitative analysis of BrdU/Bcl-2 double-positive cells were 0% at 7 days, 15.8 ± 3.2% at 14 days, 79.1 ± 10.3% at 21 days, and 88.6 ± 7.0% at 30 days (Fig. 2D,E). These findings indicated that human-*bcl-2* gene expression under the control of the NSE promoter began at the immature neuronal stage and remained constant in surviving mature neurons.

Progenitor Cell Proliferation, Survival, and Differentiation in NSE-bcl-2 Transgenic Mice

There were no significant differences in any of the parameters including cerebral blood flow, rectal and skull temperatures between both groups during and after transient forebrain ischemia (data not shown). Under normal conditions, no significant differences between NSE-*bcl-2* transgenic mice (18.5 ± 8.0/mm^2) and wild-type littermates (19.5 ± 10.8/mm^2) were observed in the number of BrdU-positive cells at 1 day after BrdU administration (Fig. 3A). Survival of progenitor cells was examined 30 days after BrdU administration. The numbers of BrdU-positive cells were 4.5 ± 3.5/mm^2 in wild-type littermates and 9.5 ± 7.1/mm^2 in NSE-*bcl-2* transgenic mice (Fig. 3A). Compared to the values obtained at Day 1, the number of surviving BrdU-positive cells was greater in NSE-*bcl-2* transgenic mice (51%) than in wild-type littermates (24%), with an approximate 25% increase. The numbers of BrdU/NeuN double-positive cells were 4.0 ± 2.8/mm^2 in wild-type littermates and 8.4 ± 5.6/mm^2 in NSE-*bcl-2* transgenic mice. The ischemic neuronal damage in the hilus was of similar severity between NSE-*bcl-2* transgenic mice and wild-type littermates, and the survival of newborn granule neurons was not associated with the degree of the injury of the CA1 sector (data not shown). After ischemia, the number of BrdU-positive cells at Day 1 did not differ between NSE-*bcl-2* transgenic mice (100.5 ± 21.1/mm^2) and wild-type littermates (110.9 ± 15.8/mm^2). The number of BrdU-positive cells 1 day after BrdU labeling was not different between both groups at 39 days (10.8 ± 7.4/mm^2 in wild-type littermates; 8.2 ± 6.8/mm^2 in NSE-*bcl-2* transgenic mice) after ischemia. In contrast, NSE-*bcl-2* transgenic mice (65.7 ± 26.7/mm^2) showed a significant increase in the number of BrdU-positive cells in the SGZ and GCL compared to that in wild-type littermates (41.0 ± 17.6/mm^2), an approximate 30% increase in survival rate (Fig. 3B). Moreover, the number

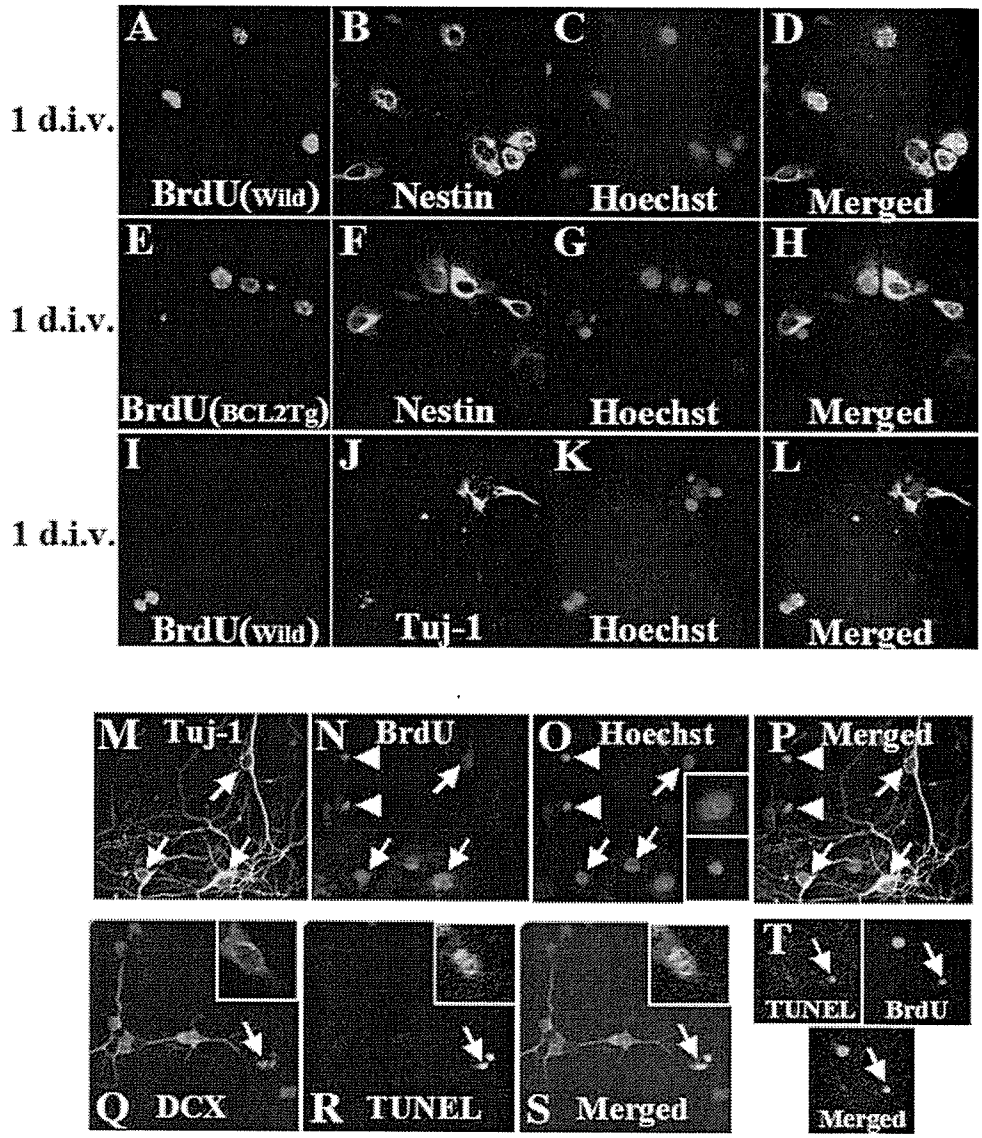

Fig. 5. BrdU (red), nestin (green), and Hoechst 33285 (blue) fluorescence of wild-type littermates (**A–D**) and NSE-*bcl-2* transgenic mice (**E–H**) at 1 day after seeding were shown. A merged image of (D) and (H) depicts BrdU/nestin/Hoechst. **I–L:** BrdU, Tuj-1, and Hoechst fluorescence at 1 day were visualized. **M–P:** Nuclear morphology of BrdU-positive newborn cells in primary culture 14 days after seeding visualized by Hoechst staining. Nuclear morphology with healthy-looking chromatin structure in BrdU/Tuj-1 double-positive cells (arrows) was visualized by Hoechst (O, right insets, upper panel). In contrast, some of BrdU-positive newborn neurons had fragmented and condensed nuclei (arrowheads) (O, right insets, bottom panel). **Q–S:** DCX and TUNEL fluorescence were shown (DCX/TUNEL double-positive cells; arrow). **T:** TUNEL/BrdU double-positive cells (arrows) were visualized.

of BrdU/NeuN double-positive cells in NSE-*bcl-2* transgenic mice (56.5 ± 18.7/mm^2) was significantly increased than that in wild-type littermates (36.1 ± 12.3/mm^2).

To assess the contribution of apoptotic cell death to the progressive reduction, we used double-immunolabeling with anti-BrdU antibody and TUNEL staining. Some of BrdU-positive cells showed colocalization of TUNEL staining (Fig. 3C, arrow). Under ischemic condition, the number of BrdU/TUNEL double-positive cells in NSE-*bcl-2* transgenic mice (0.3 ± 0.1/section, n = 10) was significantly decreased than that in wild-type littermates (2.3 ± 1.0/section, n = 10) (Fig. 3C,D). This finding suggests that ischemia promotes the proliferation of newborn cells. Followed by the increased number of death of newborn cells, however, Bcl-2 overexpression enhanced survival of those newborn neurons.

Under both conditions, no significant differences were observed in the percentages of BrdU/NeuN double-positive cells and BrdU/GFAP double-positive cells in the SGZ and GCL between the groups at 30 days (Fig. 4A). Under ischemic conditions, no significant differences were observed in progenitor cell differentiation (data not shown). There was no significant difference in the total volume of the hippocampal CA1 sector in the 18-month-old mouse. On the other hand, the total volume of cells in the DG in NSE-*bcl-2* transgenic mice was significantly greater than that of wild-type littermates. These data provide additional evidence consistent with the reduced cell death by Bcl-2 transgene (Fig. 4B).

Enhanced Survival of Newborn Neurons From NSE-bcl-2 Transgenic Mice in Neuron–Glia Mixed Culture

To directly confirm the findings that Bcl-2 enhanced survival of nascent neurons in vivo, we analyzed primary

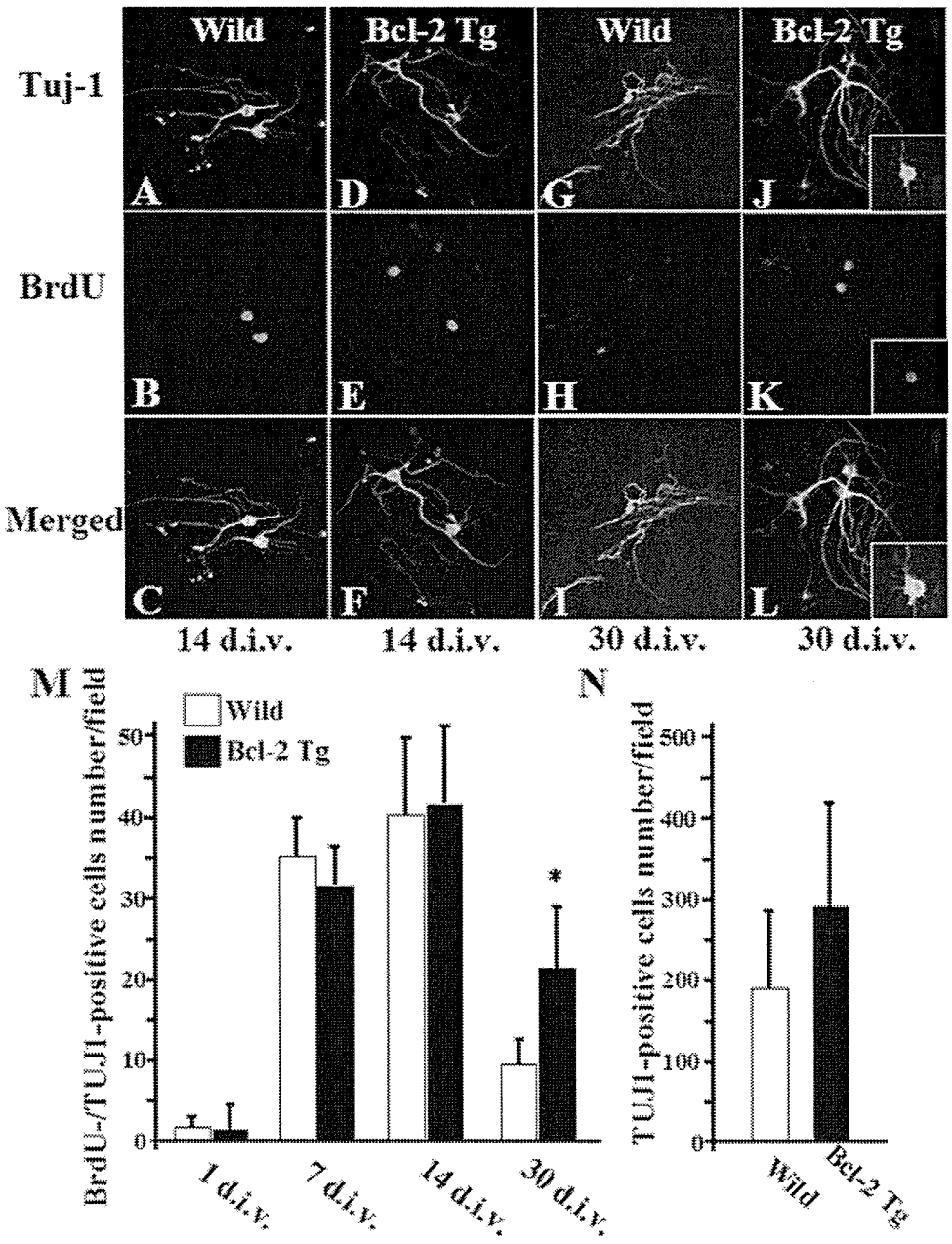

Fig. 6. Effect of Bcl-2 overexpression on survival of newborn neurons in primary neuron-glia culture. **A–L:** High-magnification confocal images are shown for Tuj1 (green) and BrdU (red) of cultured primary hippocampal neurons from wild-type littermates (A–C, G–I) and NSE-*bcl-2* transgenic mice (D–F, J–L) at 14 days (A–F) or 30 days (G–L) after seeding (L). Right insets in (J–L) show Bcl-2 immunofluorescence (green) in BrdU-positive hippocampal neurons (red) from NSE-*bcl-2* transgenic mice at 30 days. The number of Tuj1/BrdU double-positive cells (**M**) and the total number of BrdU-positive cells (**N**) at 30 days (n = 8). $*P < 0.05$ vs. control. Figure can be viewed in color online via www.interscience.wiley.com.

hippocampal cultures from P0 mice with BrdU labeling. In our hippocampal cultures, >90% of BrdU-positive cells were positive for the precursor cell marker nestin in wild-type littermates and in NSE-*bcl-2* transgenic mice at 1 day after seeding (Fig. 5A–H). In contrast, only a few BrdU-positive cells showed expression for the neuronal marker Tuj1 at 1 day (Fig. 5I–L). The nuclear morphology of neurons was examined after staining the cell nuclei with Hoechst 33285 dye. Newborn neuronal identity of the cells was shown by double-labeling for BrdU and Tuj-1. After 14 days, many BrdU/Tuj-1 double-positive newborn neurons displayed typical, healthy-looking, chromatin structure (Fig. 5M–P, arrows). Some of newborn neurons had fragmented and condensed nuclei (Fig. 5M–P, arrowheads). Moreover, some of DCX-positive immature neurons were TUNEL-positive (Fig. 5Q–S, arrowheads). No differences between two groups were observed in the numbers of cultured BrdU/Tuj-1 double-positive new neurons at 1, 7, or 14 days after seeding (Fig. 6A–L). In contrast, NSE-*bcl-2* transgenic mice showed a significant increase in the numbers of cultured BrdU/Tuj-1 double-positive cells compared to the numbers of wild-type littermates at 30 days (1, 7, 14, and 30 days in wild-type: 1.8 ± 0.1, 36.2 ± 3.3, 41.1 ± 9.0, 9.8 ± 3.1, respectively; in NSE-*bcl-2* transgenic mice: 1.6 ± 0.4, 30.8 ± 3.4, 42.4 ± 9.6, 22.3 ± 7.3, respectively) (Fig. 6M). There was an

increase in the total number of Tuj1-positive neurons in NSE-*bcl-2* transgenic mice at 30 days ($P = 0.09$) (Fig. 6N). These results showed that Bcl-2 expression promotes survival of cultured newborn neurons.

DISCUSSION

The present findings provide insight into the role of Bcl-2 in adult neurogenesis. Consistent with previous studies (Young et al., 1999), most newborn cells, a mixed population of immature and mature neurons, die via apoptosis. It has been reported recently that in the adult mouse olfactory bulb, Days 14–28 after the generation are a critical period for the survival of new granule cells, and during that time they become susceptible to apoptotic cell death (Yamaguchi and Mori, 2005). This study shows that almost the same time-point was crucial for the survival of newborn neurons in the adult hippocampus under ischemic conditions.

In the CNS, Bcl-2 is expressed highly during neurogenesis in the developing brain. Bcl-2 plays important roles in the regulation of neuronal death during development and the early postnatal period (Martinou et al., 1994). Moreover, in the hippocampal dentate gyrus, Bcl-2 expression is high not only during development but also in adulthood (Merry et al., 1994).

Consistent with the study by Fujioka et al. (2004), we also observed that, in addition to mature granule cells, newborn immature neurons in the dentate gyrus of *bcl-2* transgenic mice under the NSE promoter expressed human Bcl-2 immunoreactivity (Fig. 2). Aged NSE-*bcl*-2 transgenic mice possess supernumerary neurons in the dentate gyrus, but not in the CA1 and CA2 subregions. Based on these findings, we used NSE-*bcl*-2 transgenic mice to elucidate the role of Bcl-2 in adult neurogenesis.

TUNEL staining indicates simply DNA damage, but it is not a specific marker of apoptosis. Therefore, we must interpret TUNEL staining vigilantly. BrdU labeling is necessary, but not sufficient, to prove that a given cell has divided. Bauer and Patterson (2005) showed recently that BrdU is not incorporated significantly during DNA repair in three models of injury-induced neuronal apoptosis.

Cerebral ischemia leads to markedly enhanced proliferation of neuronal progenitor cells (Liu et al., 1998; Yagita et al., 2001). However, only a small fraction of these newborn neurons survive. We observed that ischemia induced a similar increase in both BrdU-positive cells and BrdU/TUNEL double-positive cells in the hippocampal dentate gyrus. The present study suggests that ischemia simultaneously increases both neurogenesis and neuronal elimination and that Bcl-2 is important for the long-term survival of newborn neurons in hippocampal neurogenesis after ischemia. Additionally, the Bcl-2 family has been shown to be important for protection from focal and global ischemia (Martinou et al., 1994; Kitagawa et al., 1998). The ability to upregulate Bcl-2 expression may lead to the development of brain protection and repair strategies for the treatment of brain ischemia.

In summary, this study shows that Bcl-2 overexpression increases survival of newly generated neurons in the hippocampal dentate gyrus under normal and ischemic conditions. These results indicate that modulation of Bcl-2 levels may have implications for therapeutic intervention to enhance neurogenesis for functional restoration, particularly after ischemia.

ACKNOWLEDGMENTS

The authors thank A. Kanzawa and S. Higa for secretarial assistance. T. Sasaki is a research fellow of the Japan Society of the Promotion of Science.

REFERENCES

Abe-Dohmae S, Harada N, Yamada K, Tanaka R. 1993. Bcl-2 gene is highly expressed during neurogenesis in the central nervous system. Biochem Biophys Res Commun 191:915–921.

Adams JM, Cory S. 1998. The Bcl-2 protein family: arbiters of cell survival. Science 281:1322–1326.

Arvidsson A, Collin T, Kirik D, Kokaia Z, Lindvall O. 2002. Neuronal replacement from endogenous precursors in the adult brain after stroke. Nat Med 8:963–970.

Bauer S, Patterson PH. 2005. The cell cycle-apoptosis connection revisited in the adult brain. J Cell Biol 171:641–650.

Bayer SA. 1980. Development of the hippocampal region in the rat. I. Neurogenesis examined with 3H-thymidine autoradiography. J Comp Neurol 190:87–114.

Chen J, Graham SH, Nakayama M, Zhu RL, Jin K, Stetler RA, Simon RP. 1997. Apoptosis repressor genes Bcl-2 and Bcl-x-long are expressed in the rat brain following global ischemia. J Cereb Blood Flow Metab 17: 2–10.

Fujioka T, Fujioka A, Duman RS. 2004. Activation of cAMP signaling facilitates the morphological maturation of newborn neurons in adult hippocampus. J Neurosci 24:319–328.

Gould E, Cameron HA. 1996. Regulation of neuronal birth, migration and death in the rat dentate gyrus. Dev Neurosci 18:22–35.

Kempermann G, Gast D, Kronenberg G, Yamaguchi M, Gage FH. 2003. Early determination and long-term persistence of adult-generated new neurons in the hippocampus of mice. Development 130:391–399.

Kitagawa K, Matsumoto M, Tsujimoto Y, Ohtsuki T, Kuwabara K, Matsushita K, Yang G, Tanabe H, Martinou JC, Hori M, Yanagihara T. 1998. Amelioration of hippocampal neuronal damage after global ischemia by neuronal overexpression of BCL-2 in transgenic mice. Stroke 29:2616–2621.

Liu J, Solway K, Messing RO, Sharp FR. 1998. Increased neurogenesis in the dentate gyrus after transient global ischemia in gerbils. J Neurosci 18:7768–7778.

Martinou JC, Dubois-Dauphin M, Staple JK, Rodriguez I, Frankowski H, Missotten M, Albertini P, Talabot D, Catsicas S, Pietra C, et al. 1994. Overexpression of BCL-2 in transgenic mice protects neurons from naturally occurring cell death and experimental ischemia. Neuron 13: 1017–1030.

Merry DE, Veis DJ, Hickey WF, Korsmeyer SJ. 1994. bcl-2 protein expression is widespread in the developing nervous system and retained in the adult PNS. Development 120:301–311.

Pencea V, Bingaman KD, Wiegand SJ, Luskin MB. 2001. Infusion of brain-derived neurotrophic factor into the lateral ventricle of the adult rat leads to new neurons in the parenchyma of the striatum, septum, thalamus, and hypothalamus. J Neurosci 21:6706–6717.

Sasaki T, Kitagawa K, Sugiura S, Omura-Matsuoka E, Tanaka S, Yagita Y, Okano H, Matsumoto M, Hori M. 2003. Implication of cyclooxygenase-2 on enhanced proliferation of neural progenitor cells in the adult mouse hippocampus after ischemia. J Neurosci Res 72:461–471.

van Praag H, Kempermann G, Gage FH. 1999. Running increases cell proliferation and neurogenesis in the adult mouse dentate gyrus. Nat Neurosci 2:266–270.

van Praag H, Schinder AF, Christie BR, Toni N, Palmer TD, Gage FH. 2002. Functional neurogenesis in the adult hippocampus. Nature 415:1030–1034.

Yagita Y, Kitagawa K, Ohtsuki T, Takasawa K, Miyata T, Okano H, Hori M, Matsumoto M. 2001. Neurogenesis by progenitor cells in the ischemic adult rat hippocampus. Stroke 32:1890–1896.

Yamaguchi M, Mori K. 2005. Critical period for sensory experience-dependent survival of newly generated granule cells in the adult mouse olfactory bulb. Proc Natl Acad Sci U S A 102:9697–9702.

Young D, Lawlor PA, Leone P, Dragunow M, During MJ. 1999. Environmental enrichment inhibits spontaneous apoptosis, prevents seizures and is neuroprotective. Nat Med 5:448–453.

Comparison of 3.0- and 1.5-T Three-dimensional Time-of-Flight MR Angiography in Moyamoya Disease: Preliminary Experience[1]

Yasutaka Fushimi, MD
Yukio Miki, MD, PhD
Ken-ichiro Kikuta, MD, PhD
Tsutomu Okada, MD
Mitsunori Kanagaki, MD, PhD
Akira Yamamoto, MD
Kazuhiko Nozaki, MD, PhD
Nobuo Hashimoto, MD, PhD
Takashi Hanakawa, MD, PhD
Hidenao Fukuyama, MD, PhD
Kaori Togashi, MD, PhD

Purpose: To prospectively compare 3.0- and 1.5-T three-dimensional (3D) time-of-flight (TOF) magnetic resonance (MR) angiography in patients with moyamoya disease, with special emphasis on the visualization of abnormal netlike vessels (moyamoya vessels).

Materials and Methods: Study protocols were approved by the local ethics committee; written informed consent was obtained from all patients. The study included 24 consecutive patients with moyamoya disease (four male and 20 female patients). Patients ranged in age from 17 to 66 years (mean age, 41 years). Moyamoya disease had been diagnosed in all patients before they were entered into the study. All patients underwent 3D TOF MR angiography at both 3.0 and 1.5 T; imaging examinations were performed within 14 days of each other. Maximum intensity projections (MIPs) obtained with MR angiography performed at both 3.0 and 1.5 T were evaluated by two neuroradiologists; the visualization of moyamoya vessels was graded according to a 4-point scale. For both 3.0- and 1.5-T imaging, the number of high-signal-intensity areas and the summation of cross-sectional areas of high signal intensity on source images obtained at the same level of MR angiography were compared quantitatively by using the Wilcoxon matched-pair signed-rank test.

Results: Moyamoya vessels were better visualized on MIPs obtained with 3.0-T imaging than on MIPs obtained with 1.5-T imaging ($P < .001$). At the identical level of the source image, 3.0-T imaging depicted more high-signal-intensity areas than did 1.5-T imaging. Wider cross-sectional areas of moyamoya vessels were visualized with 3.0-T imaging than with 1.5-T imaging ($P < .001$).

Conclusion: Moyamoya vessels are better depicted with MR angiography at 3.0 T than at 1.5 T.

[1] From the Department of Diagnostic Imaging and Nuclear Medicine (Y.F., Y.M., T.O., M.K., A.Y., K.T.), Department of Neurosurgery (K.K., K.N., N.H.), and Human Brain Research Center (T.H., H.F.), Kyoto University Graduate School of Medicine, 54 Shogoin-Kawaharacho, Sakyo-ku, Kyoto, 606-8507, Japan. From the 2005 RSNA Annual Meeting. Received November 29, 2004; revision requested January 20, 2005; revision received April 3; final version accepted May 2. Supported in part by a grant from the Ministry of Education Culture, Sports, Science and Technology, Japan. **Address correspondence to** Y.M. (e-mail: *mikiy@kuhp.kyoto-u.ac.jp*).

Moyamoya disease is a rare cerebrovascular occlusive disease of unknown origin and is characterized by stenosis or occlusion of both internal carotid arteries (ICAs) at the supraclinoid portion (1,2). Although this disease occurs predominantly in Asian populations, particularly in Japan, it has also been reported in other countries (3–5). The major symptoms of moyamoya disease are related to age, with transient ischemic attack often seen in pediatric patients and intracranial hemorrhage often seen in adults.

The principal angiographic feature of moyamoya disease is bilateral stenosis or occlusion of the supraclinoid portions of the ICAs, potentially extending to the proximal portions of the anterior cerebral arteries and middle cerebral arteries (MCAs), with the presence of abnormal netlike vessels (moyamoya vessels) in the basal areas (1). Leptomeningeal collateral vessels from the posterior cerebral arteries or transdural collateral vessels from the external carotid arteries may also be present (1).

With the development of magnetic resonance (MR) imaging techniques, the diagnosis of moyamoya disease with MR imaging and MR angiography has become possible (6). When ICA occlusion and moyamoya vessels are demonstrated at MR angiography, conventional angiography is unnecessary, particularly in pediatric patients (6). Interpretation of high-quality images is crucial when diagnosing moyamoya disease with MR imaging without conventional angiography. Precise evaluation of abnormal vascular networks in the basal ganglia, in addition to vascular occlusion, is essential for securing a definitive diagnosis of moyamoya disease (6–8).

MR imaging techniques with 3.0-T imaging have gradually become prevalent. Imaging at 3.0 T provides a better signal-to-noise ratio, which increases approximately linearly with constant magnetic induction field from 1.5- to 3.0-T imaging (9,10). The T1 relaxation time increases at higher magnetic field strengths, and this produces improved vessel-tissue contrast at 3.0-T imaging (11–13). A better signal-to-noise ratio and increased T1 relaxation time at 3.0-T imaging contribute to the improved quality of MR angiography. Furthermore, Willinek et al (14) demonstrated that, in the diagnosis of cerebrovascular occlusive disease, high-spatial-resolution three-dimensional (3D) time-of-flight (TOF) MR angiography at 3.0 T is superior to that at 1.5 T. To our knowledge, however, no reports have focused on the comparison of 3.0- and 1.5-T MR angiography in patients with moyamoya disease.

Thus, the purpose of our study was to prospectively compare 3.0- and 1.5-T 3D TOF MR angiography in patients with moyamoya disease, with special emphasis on the visualization of moyamoya vessels.

Scores in the Depiction of Moyamoya Vessels

Patient No.	1.5-T Field Strength	3.0-T Field Strength
1	2	3
2	2	3
3	1	2
4	2	3
5	2	2
6	2	2
7	3	3
8	1	2
9	2	3
10	2	2
11	3	3
12	3	3
13	2	3
14	2	3
15	2	3
16	1	3
17	2	3
18	2	3
19	2	3
20	1	3
21	1	3
22	2	3
23	3	3
24	1	3

Note.—Scores used in the depiction of moyamoya vessels are as follows: 3 = excellent (vessel segments were clearly and continuously visualized, and vessel-tissue contrast is high), 2 = visible (vessel segments are visualized and adequate for a confident diagnosis, but vessel-tissue contrast is not particularly high), 1 = scarcely visible (vessel segments were visualized but inadequate for diagnosis), and 0 = not visible.

Materials and Methods

Study Design and Patients

A prospective study was performed with 24 consecutive patients with moyamoya disease (four male and 20 female patients) between December 2003 and September 2004. Moyamoya disease had been diagnosed in all patients with conventional angiography before they were entered into our study (6). The mean patient age was 41 years (age range, 17–66 years). Patients were initially suspected of having moyamoya disease due to transient ischemic attack or cerebral infarction (n = 14), intracranial hemorrhage (n = 9), or incidental findings at MR imaging after a traffic accident (n = 1). Of the 24 patients, seven (29%) had not undergone any surgical synangiosis procedure. Seventeen of the 24 patients (71%) had undergone creation of a superficial temporal artery (STA)–MCA anastomosis combined with encephalomyosynangiosis (n = 15) or encephaloduroarteriosynangiosis (n = 2). All patients had undergone regular follow-up. In these 17 patients, the mean postoperative duration at the time of our study was 89 months (range, 7–288 months).

Study protocols were approved by the local ethics committee, and all pa-

Published online before print
10.1148/radiol.2383042020

Radiology 2006; 239:232–237

Abbreviations:
ICA = internal cerebral artery
MCA = middle cerebral artery
MIP = maximum intensity projection
STA = superficial temporal artery
3D = three dimensional
TOF = time of flight

Author contributions:
Guarantors of integrity of entire study, all authors; study concepts/study design or data acquisition or data analysis/interpretation, all authors; manuscript drafting or manuscript revision for important intellectual content, all authors; approval of final version of submitted manuscript, all authors; literature research, Y.M., K.K., M.K., A.Y., K.N., T.H., H.F.; clinical studies, Y.F., K.K., T.O., K.N., T.H., H.F.; statistical analysis, Y.F., Y.M., M.K., A.Y., K.N., N.H., H.F., K.T.; and manuscript editing, Y.F., Y.M., T.O., N.H., H.F., K.T.

Authors stated no financial relationship to disclose.

tients provided written informed consent before entering the study. When the patient was a minor, additional written informed consent was also obtained from the parent.

MR Imaging

Our study was performed with 3.0-T (Magnetom Trio; Siemens, Erlangen, Germany) and 1.5-T (Magnetom Symphony; Siemens) MR units. Circular polarized head coil arrays were used for both MR units. The following parameters were used for 3.0-T MR angiography: 22.0/3.7 (repetition time msec/echo time msec), 20° flip angle, 0.8-mm-thick sections, 200 × 200-mm field of view with a 512 × 208 matrix, effective voxel size of 0.39 × 0.96 × 0.8 mm, and acquisition time of 5 minutes 51 seconds. The following parameters were used for 1.5-T MR angiography: 35/7, 0.8-mm-thick sections, 20° flip angle, 200 × 200-mm field of view with a 512 × 208 matrix, effective voxel size of 0.39 × 0.96 × 0.8 mm, and acquisition time of 6 minutes 21 seconds. The repetition time and echo time could not be matched because of the limitations of specific absorption rate with the 3.0-T MR system.

Image Analysis

Transverse and lateral maximum intensity projections (MIPs) obtained with 3.0- and 1.5-T MR angiography were independently assessed by two neuroradiologists (Y.F. and Y.M., with 8 and 19 years of experience, respectively). Lateral MIPs were reconstructed with data from the ipsilateral hemisphere. To evaluate the visibility of moyamoya vessels under identical circumstances, we evaluated only transverse and bilateral MIP images instead of reviewing all the angles of MIP images. The visibility of moyamoya vessels was assessed and scored as follows: 3, excellent (vessel segments were clearly and continuously visualized, and vessel-tissue contrast appears to be high); 2, visible (vessel segments are visualized and adequate for a confident diagnosis, but vessel-tissue contrast does not appear to be particularly high); 1, scarcely visible (vessel segments were visualized but inadequate for diagnosis); and 0, not visible. Readers were blinded to field strength; discrepancies between the two readers were resolved by consensus. A consensus reading was required in one patient for 3.0-T images (4.2%) and in three patients for 1.5-T images (12.5%).

A particle-counting method was used for source images from MR angiography. With use of ImageJ software, a

Figure 1

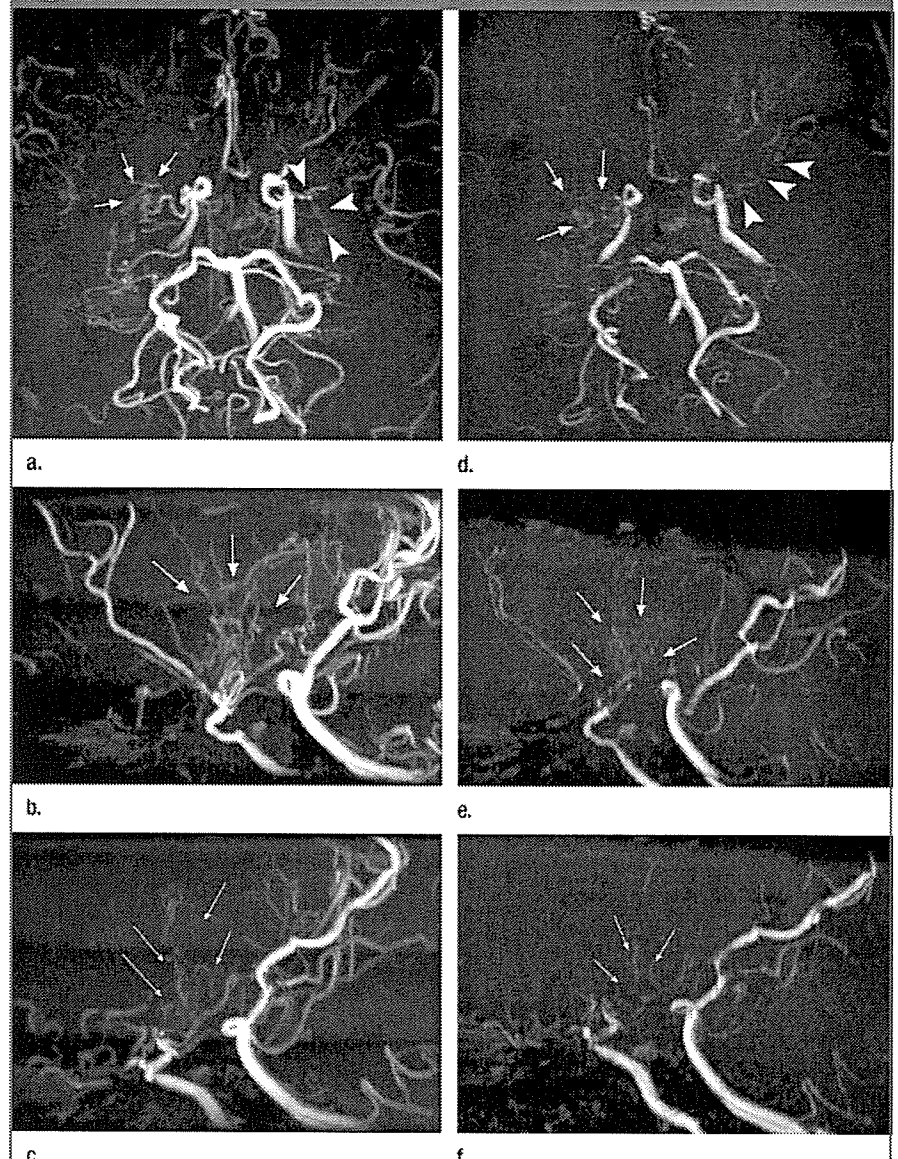

Figure 1: MIPs from 3D TOF MR angiography in a 58-year-old woman show moyamoya vessels (arrows) from ICAs. **(a)** Transverse MIP, **(b)** lateral MIP of the right side, and **(c)** lateral MIP of the left side from 3.0-T MR angiography (22.0/3.7). **(d)** Transverse MIP, **(e)** lateral MIP of the right side, and **(f)** lateral MIP of the left side from 1.5-T MR angiography (35/7). Transverse MIPs reveal more moyamoya vessels on the right side from the right ICA than on the left side. Moyamoya vessels from the right ICA are more clearly seen with 3.0-T imaging than with 1.5-T imaging. On the left side, 1.5-T MR angiography shows slight and discontinuous moyamoya vessels (arrowheads in **d**), whereas 3.0-T MR angiography shows fine moyamoya vessels (arrowheads in **a**) continuously and more clearly. MIPs from 3.0-T imaging were scored as 3 (excellent) and those from 1.5-T imaging were scored as 2 (visible).

Java-based image analysis program developed at the U.S. National Institutes of Health (*http://rsb.info.nih.gov/ij/index.html*), high signal intensity in the basal ganglia of the anterior circulation, which correspond to moyamoya vessels (1), were manually selected and semiautomatically counted by one neuroradiologist (Y.F.). Image selection from 3.0- and 1.5-T MR angiographic data obtained in the same patient was performed simultaneously, as identical section levels can be selected; this enabled comparison of images obtained at 3.0 and 1.5 T. Image selection procedures were performed with two personal computers by using ExaVision Lite software (Ziosoft, Tokyo, Japan). Regions of interest were carefully selected in bilateral basal ganglia without including any cisternal structures because major branches of anterior cerebral arteries and MCAs are located in the interhemispheric fissure and sylvian fissure, respectively. We determined the threshold for the source images with MR angiography to make the brightest part of brain parenchyma just black out to minimize the variances of the thresholds and obtained the binary data from MR angiography. The number of high signal intensities and the summation of cross-sectional areas of high signal intensity, which correspond to the cross-sectional area of moyamoya vessels, were obtained for 3.0- and 1.5-T imaging.

Statistical Analysis

For statistical evaluation, scores for MIPs obtained with MR angiography, the number of high-signal-intensity areas, and the summation of cross-sectional areas of high signal intensity were compared by using the Wilcoxon matched-pair signed-rank test with software (JMP 5.0; SAS Institute, Cary, NC). This was done because the Shapiro-Wilk test was performed for normality and the null hypothesis rejected. A P value of less than .05 was considered to indicate a statistically significant difference.

Figure 2

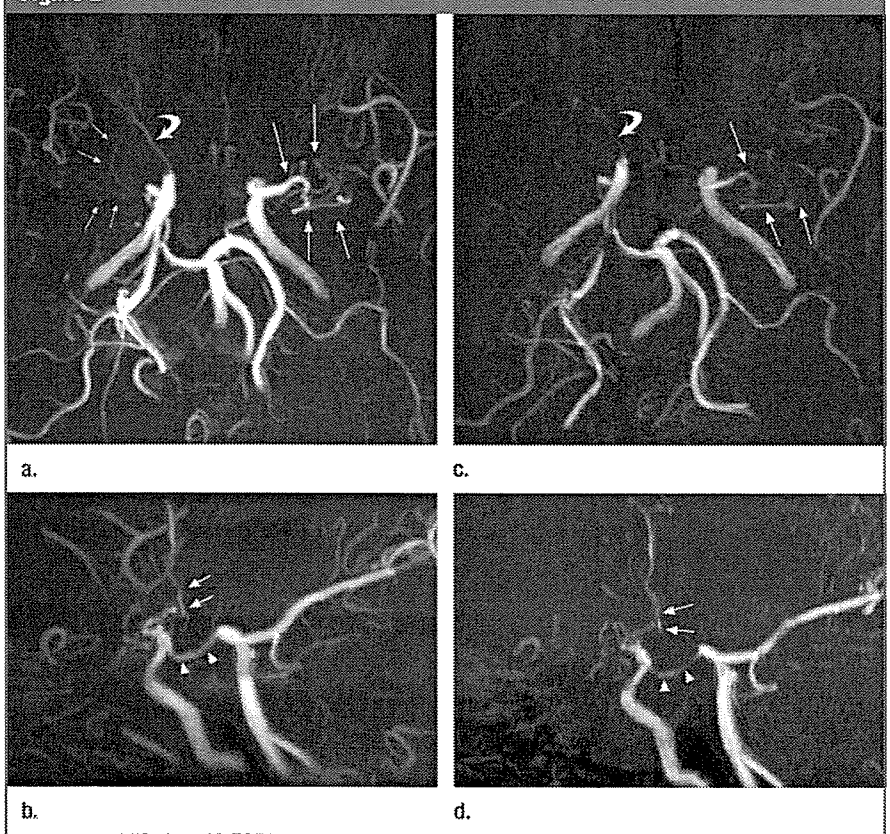

Figure 2: MIPs from 3D TOF MR angiography in a 49-year-old man. **(a)** Transverse MIP and **(b)** lateral MIP of the left side from MR angiography (22.0/3.7). **(c)** Transverse MIP and **(d)** lateral MIP of the left side from 1.5-T MR angiography (35/7). Images obtained at 3.0 T reveal prominent moyamoya vessels on the left side (long straight arrows in **a**, arrows in **b**) and scarce moyamoya vessels on the right side (short straight arrows in **a**). Images obtained at 1.5 T show moyamoya vessels on the left side (straight arrows in **c**, arrows in **d**) but no apparent moyamoya vessels on the right side. Note that the posterior communicating artery (arrowheads in **b** and **d**) and right ophthalmic artery (curved arrow in **a** and **c**) are visualized more clearly at 3.0 T than at 1.5 T. MIPs from 3.0-T imaging were scored as 3 (excellent), whereas images obtained at 1.5 T were scored as 2 (visible).

Results

MIPs were obtained with 3D TOF MR angiography in the 24 patients (Table) (Figs 1, 2). MIPs from 3.0-T MR angiography depicted moyamoya vessels more clearly than did those from 1.5-T MR angiography ($P < .001$).

The number of high-signal-intensity areas in anterior circulations (anterior cerebral artery and MCA territories) on source images obtained at both 3.0 and 1.5 T showed that the number of high-signal-intensity areas at 3.0-T imaging was greater than that at 1.5-T imaging ($P < .001$) (Figs 3, 4). Cross-sectional areas of high-signal-intensity were larger at 3.0-T imaging than at 1.5-T imaging ($P < .001$) (Fig 5).

Discussion

Our results demonstrate that moyamoya vessels are better depicted with MIPs from 3.0-T MR angiography than with those from 1.5-T MR angiography. More moyamoya vessels (in both number and cross-sectional area) were detected at 3.0-T imaging than at 1.5-T imaging. The particle-counting method with use of ImageJ software has been applied to cell counting in biologic studies (15,16). In our study, we used this method in the postprocessing of MR angiographic data to assess moyamoya vessels. This method may be useful for objective and longitudinal evaluations

Figure 3

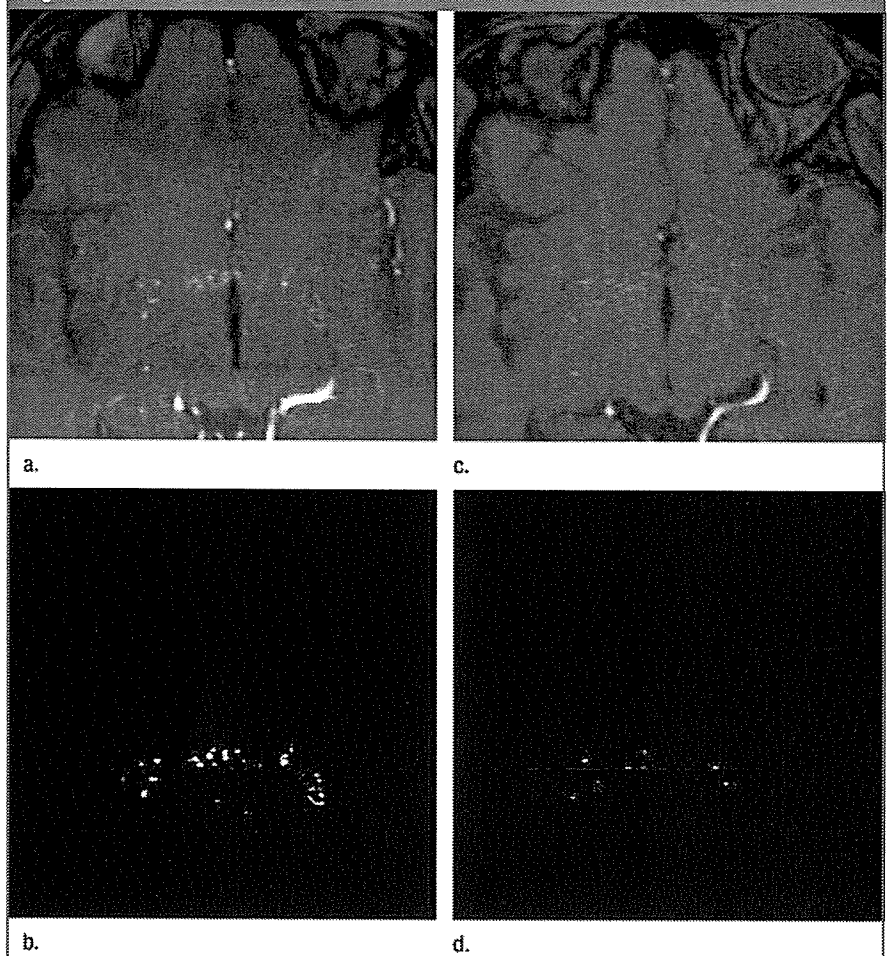

Figure 3: Images obtained in a 58-year-old woman. Source images from MR angiography obtained at the same level at **(a)** 3.0 T (22.0/3.7) and **(c)** 1.5 T (35/7). More high-signal-intensity areas in both basal ganglia were seen at 3.0-T imaging than at 1.5-T imaging. The area of anterior circulation was selected and changed into binary data. The number of high-signal-intensity areas was calculated semiautomatically, and the total number of cross-sectional areas of high signal intensity was calculated by using software. **(b)** Binary data image obtained at 3.0 T shows more high-signal-intensity areas than **(d)** data from the source image obtained at 1.5 T.

Figure 4

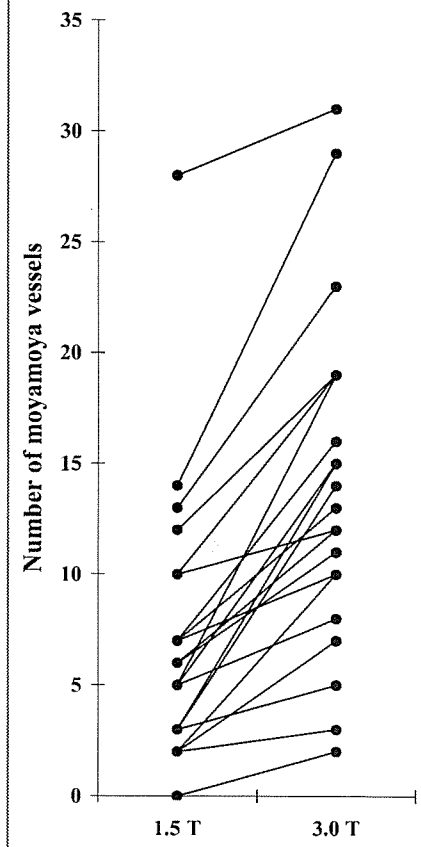

Figure 4: Graph shows the number of moyamoya vessels visualized at 3.0- and 1.5-T imaging. The moyamoya vessels were counted semiautomatically on MR angiography source images obtained at the same levels. More high-signal-intensity areas were seen at 3.0 T than at 1.5 T.

because the number and cross-sectional area of moyamoya vessels are provided.

Moyamoya disease is a rare cerebrovascular disease. In adult patients, intracerebral hemorrhage is one of the most common complications at disease onset (17–20). For patients with moyamoya disease and hemorrhage, repeat bleeding is the most crucial event that affects quality of life (21,22). The mechanisms of repeat bleeding supposedly involve rupture of moyamoya vessels. Moyamoya vessels have a tendency to contract; when that happens, the remaining moyamoya vessels receive more pressure, which leads to vessel rupture (18). Thus, observation of the appearance of moyamoya vessels at periodic follow-up MR angiography is clinically important (23,24). The results of our study demonstrate that more information about moyamoya vessels can be obtained with 3.0-T MR angiography than with 1.5-T MR angiography. This enables more precise evaluation of moyamoya vessels with regard to factors such as stenosis, dilatation, and increases or decreases in number. Our study was a preliminary study that targeted moyamoya disease. To our knowledge, this is the first study in which the visibility of moyamoya vessels has been described at both 3.0- and 1.5-T MR angiography.

One limitation of our study is that most of our patients (71%) had undergone surgical treatment. After bypass surgery (creation of STA-MCA anastomosis, encephalomyosynangiosis, and encephaloduroarteriosynangiosis), collateral arteries develop from the external cerebral artery and the amount of moyamoya vessels decreases in about 50% of patients (8). In our study, only seven patients had not undergone surgery; thus, a more precise interpretation of our results would be to say that